Electron structure of the magnetopause boundary layer: Cluster/Double Star observations

M.W. Dunlop, M. G. Taylor, Y. Bogdanova, Chao Shen, Frederic Pitout, Z. Pu, J. A. Davies, Q. Zhang, J. Wang, B. Lavraud, et al.

Electron structure of the magnetopause boundary layer: Cluster/Double Star observations

M. W. Dunlop,[1,2] M. G. G. T. Taylor,[3] Y. V. Bogdanova,[4] C. Shen,[5] F. Pitout,[6] Z. Pu,[7] J. A. Davies,[1] Q.-H. Zhang,[8] J. Wang,[7] B. Lavraud,[9] A. N. Fazakerley,[4] A. Walsh,[4] C. J. Owen,[4] H. Laakso,[3] Q.-G. Zong,[7] Z.-X. Liu,[5] C. P. Escoubet,[3] C. M. Carr,[2] and H. Rème[9]

[1]   We present a comparison of two events, monitored by the Double Star and Cluster spacecraft at separate locations on the dayside magnetopause, which exhibit distinct properties at high and low latitudes in the magnetopause boundary layer during the occurrence of low-latitude reconnection. On 6 April 2004, the four Cluster and TC-1 spacecraft were on near-coincident, outbound transits of the dawnside magnetosphere at north and south midlatitudes, respectively. The observations show a series of oppositely directed flux transfer events (FTEs), fed by a low-latitude reconnection line located between the spacecraft. Although both spacecraft locations were nearly equidistant from the active reconnection region, the associated magnetopause boundary layer was maintained at TC-1 but not at Cluster. We suggest an asymmetric north and south extent of the LLBL so as to be more extensive at TC-1, where the local magnetic shear across the magnetopause is small. On 4 January 2005, the Cluster and TC-1 spacecraft all repeatedly traverse the northern, duskside magnetopause almost simultaneously, before and after a strong reversal in the IMF from northward to southward during a period of turbulent solar wind. Open flux tubes are observed within minutes of the southward turning, arising from the sudden formation of a nearby subsolar reconnection line. Before the IMF change, a complex and energized boundary layer, largely absent at the lower latitudes of TC-1, and containing an energetic (>40 keV) electron population of locally trapped and field-aligned distributions, is present at the high-latitude Cluster locations. Following reconnection onset after the IMF reversal, the boundary layer is seen to extend to TC-1, and the electron distribution, which depends on position through the boundary layer, develops as an energetic, field-aligned (bistreaming) distribution. The analysis is utilizes an extended electron distribution for energies ranging from a few to 400 keV and by reordering the transition through the magnetopause to the electron distribution.

1.   Introduction

[2]   The launch of the two spacecraft Double Star mission in coordination with the quartet of Cluster spacecraft has provided the opportunity to monitor events at distinct locations on the Earth's dayside magnetopause. The magnetopause boundary layers contain modified plasma distributions and a system of electromagnetic fields and currents, which are known to depend upon the properties of the adjacent magnetosheath and on the local magnetosphere. The process of magnetic reconnection of the Earth's dayside magnetic field with the adjacent magnetosheath magnetic field [*Dungey*, 1961] readily facilitates the transfer of momentum and energy from the solar wind into the Earth's magnetosphere and is widely thought to be a dominant process occurring in the dayside boundary, whose resulting structure ultimately controls pressure balance across the

[1]SSTD, Rutherford Appleton Laboratory, Didcot, UK.
[2]Blackett Laboratory, Imperial College London, London, UK.
[3]ESA/ESTEC, Noordwijk, Netherlands.
[4]Mullard Space Science Laboratory, University College London, Dorking, UK.
[5]Centre for Space Science and Applied Research, Chinese Academy of Sciences, Beijing, China.
[6]Max-Planck Institut fur Extraterrestrische Physik, Garching, Germany.
[7]School of Earth and Space Sciences, Peking University, Beijing, China.
[8]UAPS, Polar Research Institute of China, Shanghai, China.
[9]Centre d'Etude Spatiale des Rayonnements, Toulouse, France.

boundary. Linking the local magnetic field to the upstream, interplanetary magnetic field (IMF) orientation therefore provides a global context for the influence of the solar wind on the magnetosphere-ionosphere system. Both high- and low-latitude reconnection sites are possible so that the resulting magnetopause behavior (e.g., the onset of magnetic merging) is sensitive both to magnetopause location and the prevailing conditions.

[3] Different IMF orientations or solar wind conditions give rise to varying rates of reconnection [*Crooker*, 1979] as well as variations in the location of the reconnection site [e.g., *Gosling et al.*, 1991; *Kessel et al.*, 1996; *Russell and Elphic*, 1978]. Under southward IMF the signatures of transient or bursty (sporadic) reconnection in particular are usually observed to correspond to bundles of newly reconnected magnetic flux at the subsolar region, which subsequently convect tailward in the form of tube-like structures threading the magnetopause (considered to be a flux transfer event (FTE) [*Russell and Elphic*, 1979; *Rijnbeek et al.*, 1982, 1984; *Sibeck et al.*, 1989; *Berchem and Russell*, 1984; *Smith and Lockwood*, 1996]). Under northward IMF, transient reconnection is most often observed to occur on high-latitude, lobe field lines, tailward of the cusps [e.g., *Lavraud et al.*, 2002; *Twitty et al.*, 2004; *Bogdanova et al.*, 2005; *Lavraud et al.*, 2005a]. A number of open questions on FTE occurrence and reconnection rates remain. For example, an aspect of the debate on dayside magnetic merging centers on the issue of whether antiparallel or component merging dominates the reconnection process, which in turn controls the most likely sites for X line formation. Investigations of X line formation are assisted either by direct sampling of the X line (which is relatively rare), or indirectly, by monitoring FTE and open boundary layer occurrence and location. For example, the polarity of the magnetic field signature of an FTE may be used as an indication of to which hemisphere the flux tube is connected [e.g., *Rijnbeek et al.*, 1984; *Lockwood et al.*, 2001]. This interpretation, however, is most clear only when the flux tubes are well sampled sufficiently near the subsolar region and where the magnetosheath flow is sub-Alfvenic. It is expected that FTEs will have corresponding signatures when sampled in the high-altitude cusp region and on the flanks, although the characteristic signatures could differ from dayside exterior boundary layer observations owing to the different magnetospheric field configuration at these locations [*Dunlop et al.*, 2001; *Marchaudon et al.*, 2005]. Sampling of flux tubes may also give rise to nonstandard FTE signatures [*Wang et al.*, 2006].

[4] During periods of active reconnection, associated with momentum and energy transfer, both the ion composition and the electron distribution in the magnetopause boundary layer are seen to change locally as a result of mixing of magnetospheric and magnetosheath populations and are dependent on proximity to the magnetic merging site. The low-latitude boundary layer (LLBL) has been most extensively studied [e.g., *Eastman and Hones*, 1979; *Eastman et al.*, 1996; *Paschmann*, 1979; *Fuselier et al.*, 1997; *Onsager et al.*, 2001]. The extent, morphology, and dynamics of the boundary layer is still a very active area of space plasma research. The boundary layer properties will have a characteristic ordering through the transition from magnetosphere to magnetosheath, depending on proximity to the merging site and the reconnection history (opened or closed magnetic flux). The boundary layer generally shows a complex structure with the existence of inner and outer parts of the LLBL and a magnetosheath boundary layer (MSBL) [*Le et al.*, 1996; *Fuselier et al.*, 1997; *Onsager et al.*, 2001; *Lavraud et al.*, 2005b]. Both hot bistreaming and trapped electron populations may exist on adjacent, likely magnetospheric, field lines. There is also evidence of a high degree of substructure on the magnetopause [*Song et al.*, 1993; *Hu and Sonnerup*, 2003; *Hasegawa et al.*, 2004a, 2004b]. These findings suggest that more than one mechanism may contribute to low and high BL formation [e.g., *Phan et al.*, 2005; *Lavraud et al.*, 2006].

[5] The four spacecraft, in situ measurements from the ESA Cluster mission [*Escoubet et al.*, 2001] have provided extremely detailed multipoint measurements since 2001. The recent coordination of Cluster with the Chinese Double Star mission has additionally provided a significant opportunity to simultaneously monitor the properties of the dayside boundary at multiscale locations on the magnetopause. Such simultaneous coverage over a wide range of different magnetopause sites was previously only available through fortuitous spacecraft conjunctions [e.g., *Wild et al.*, 2005, 2007]. The combined six spacecraft from the two missions, however, have provided simultaneous coverage of the high and low latitudes, cusp, and low-latitude boundary layer. Recent studies have investigated X line formation (directly and indirectly) and the development of the boundary layer at both high and low latitudes. For example, *Pu et al.* [2005, 2007] surveyed a number of direct reconnection events under large B_Y and low clock angle, finding evidence of predominantly component-driven low-latitude merging in conjunction with predominantly antiparallel high-latitude sites. The identification of oppositely moving FTEs at the Double Star TC-1 and Cluster spacecraft and detailed tracking of flux tube motion between TC-1 and Cluster along the MP was made by *Wild et al.* [2005], *Dunlop et al.* [2005], *Fear et al.* [2005], and *Wang et al.* [2007] and has been recently compared to MHD simulation results by *Berchem et al.* [2008]. Comparison of the electron boundary layer in the cusp and the low-latitude boundary layer (LLBL) under northward directed interplanetary field (IMF) has been investigated recently by *Bogdanova et al.* [2008].

[6] In this paper we present results of the analysis of two previously studied Double Star/Cluster conjunctions on 6 April 2004 [*Dunlop et al.*, 2005] and 4 January 2005 [*Wang et al.*, 2007], which are sampled simultaneously at middle and high latitudes. These events were investigated in terms of the evolution of FTEs across the dayside magnetopause but also provide a particular comparison of magnetopause properties in terms of boundary layer composition and extent, as discussed here. The former event serves as a comparative situation for a standard LLBL during southward IMF. The latter event occurs during a sudden southward turning of the IMF, resulting in a switch on of reconnection, and shows significant energization of the electron population. Here, we investigate the boundary behavior in some detail, focusing in particular on the occurrence of electron energization and on the boundary layer extent. Instrumentation is described in section 2, the data sets are presented in section 3, and analysis and

discussion is presented in section 4. We summarize the results in section 5.

2. Instrumental Arrangement

[7] The Cluster spacecraft were launched in pairs in July and August 2000 into polar orbits, each with an orbital period of 57 h and each with perigee and apogee of 4 and 19.6 Earth radii (R_E), respectively. Since the orbital plane of Cluster is fixed in the inertial frame of the Earth, apogee precesses through 24 h of local time (LT) with a 12-month periodicity. In April 2004, apogee was in the prenoon sector, near 1000 LT and in January apogee lay on the postnoon flank at ~1600 LT. In this paper we compare observations from Cluster with those from TC-1, one of the pair of Double Star spacecraft [*Liu et al.*, 2005]. The TC-1 spacecraft was launched in December 2003 into a near equatorial orbit at 28.2° inclination, with an orbital period of 27.4 h, a perigee altitude of 570 km and an apogee of 13.4 R_E.

[8] We concentrate, in this study, on data from the magnetic field and thermal plasma instruments on Cluster and TC-1 and from the energetic electron instrument on Cluster. This is facilitated by common instrumentation on the two missions. The four Cluster spacecraft and both Double Star satellites carry Fluxgate Magnetometers (FGM). Each FGM instrument comprises a pair of fluxgate magnetic field sensors mounted on an axial boom, although Double Star uses a sensor design different to that used on Cluster (for descriptions of each, see *Balogh et al.* [2001] and *Carr et al.* [2005]). We employ spin resolution (4 s) and recalibrated high-resolution magnetic field data, as appropriate and as indicated in the text. The Plasma Electron and Current Experiment (PEACE) instrument on Cluster, as discussed by *Johnstone et al.* [1997], consists of two oppositely mounted instruments each comprising two separate electron sensors: Low-Energy Electron Analyzer (LEEA) and High-Energy Electron Analyzer (HEEA). On the Double Star TC-1 the Cluster flight spare of the PEACE/LEEA sensor is mounted, while the spare PEACE/HEEA sensor is carried on the polar Double Star TC-2 spacecraft [*Fazakerley et al.*, 2005]. The PEACE instruments nominally obtain the electron distribution at spin resolution for the energy range 0.6 eV to 26 keV (for Cluster). Similarly, while the Cluster Ion Spectrometry (CIS) [*Rème et al.*, 2001] experiment on board Cluster comprises both CODIF (Composition Distribution Function) and HIA (Hot Ion Analyzer) components, TC-1 carries only the HIA instrument [*Rème et al.*, 2005], which provides three-dimensional distributions of the ions (assumed to be protons) at spin resolution. The distributions cover the energy range 0.02–38 keV/q. Energetic electron measurements, taken from the RAPID instrument [*Wilken et al.*, 1997], on Cluster, are also used in the second event and these extend the measured electron spectrum up to 400 keV.

[9] We also employ measurements taken from the ACE spacecraft [*Stone et al.*, 1998] which is orbiting the L1 libration point upstream in the solar wind. The interplanetary magnetic field (IMF) data are used at 16 s resolution and come from the Magnetic Field Experiment [*Smith et al.*, 1998]. Solar wind density and velocity come from the Solar Wind Electron Proton Alpha Monitor [*McComas et al.*,

1998] and are used with 64-s time resolution. Suitable time lags are calculated simply as the convection times from ACE to the Cluster or TC sites.

3. Results
3.1. Event of 6 April 2004

[10] We first summarize the properties of the event analyzed by *Dunlop et al.* [2005]. The spacecraft tracks in the X-Y Geocentric Solar Magnetic (GSM) plane for both Cluster spacecraft 1 and TC-1 are shown in Figure 1a for the interval 0300 to 0800 UT on 6 April 2004. Also shown are enlarged configurations of the Cluster spacecraft array, at two points along the orbit, where the interspacecraft separations were a few hundred kilometers. During the interval, the Cluster array crosses through the dayside magnetosphere to exit through the magnetopause into the magnetosheath at high northern latitudes at about 1000 LT as shown, while TC-1 passed outbound through the magnetopause, dawnward of Cluster at ~8 LT at southerly latitudes (note that the actual magnetopause crossing occurred at ~0430 UT at Cluster and about 15 min earlier at TC-1). This pass therefore corresponded to a parallel traversal through the dayside boundary layer at middle to high latitudes, adjacent to, but not through, the north/south cusps. During the interval, the solar wind conditions measured by the ACE spacecraft corresponded to a predominantly southward, and exclusively dawnward, IMF. In the core interval around the magnetopause exits, 0400–0540 UT (lagged time), the resulting IMF clock angle first decreased from around −100° to −150° at 0500 UT and subsequently increased back to ~−100°. The prevailing solar wind dynamic pressure remained between ~2 and 3 nPa. These conditions are conducive to the onset of dayside merging and using these parameters *Dunlop et al.* [2005] employed the model implemented by *Cooling et al.* [2001] to track the motion of newly reconnected flux tubes, arising from an assumed X line, across the dayside magnetopause. Figure 1b shows the result for the lowest IMF clock angle. The model uses the most probable X line orientation (direction of the merging current) for the prevailing conditions and computes the flux tube speed and direction of motion, resulting in the array of predicted tracks as shown in Figure 1. The positions of the spacecraft show that for a low-latitude X line the spacecraft would be expected to sample FTEs moving in the directions indicated.

[11] The event indeed showed an active period of reconnection, which generated a series of FTE signatures, oppositely moving away from an apparent low-latitude reconnection site lying near the subsolar point between the spacecraft locations. These FTE observations are summarized in Figure 2 (first to fourth panels), which shows magnetic field data from all four Cluster spacecraft and for the Double Star TC-1 spacecraft as a superimposed times series plot in local LMN coordinates [*Russell and Elphic*, 1978], with the boundary normals based on MVA analysis [*Sonnerup and Cahill*, 1967] at each magnetopause position as describe in the caption. The clearest FTEs in the data from both spacecraft are identified by the dashed, vertical arrows (red for northward moving FTEs at Cluster and blue for southward moving FTEs at TC-1). The Cluster spacecraft are close enough to allow confirmation of the FTE
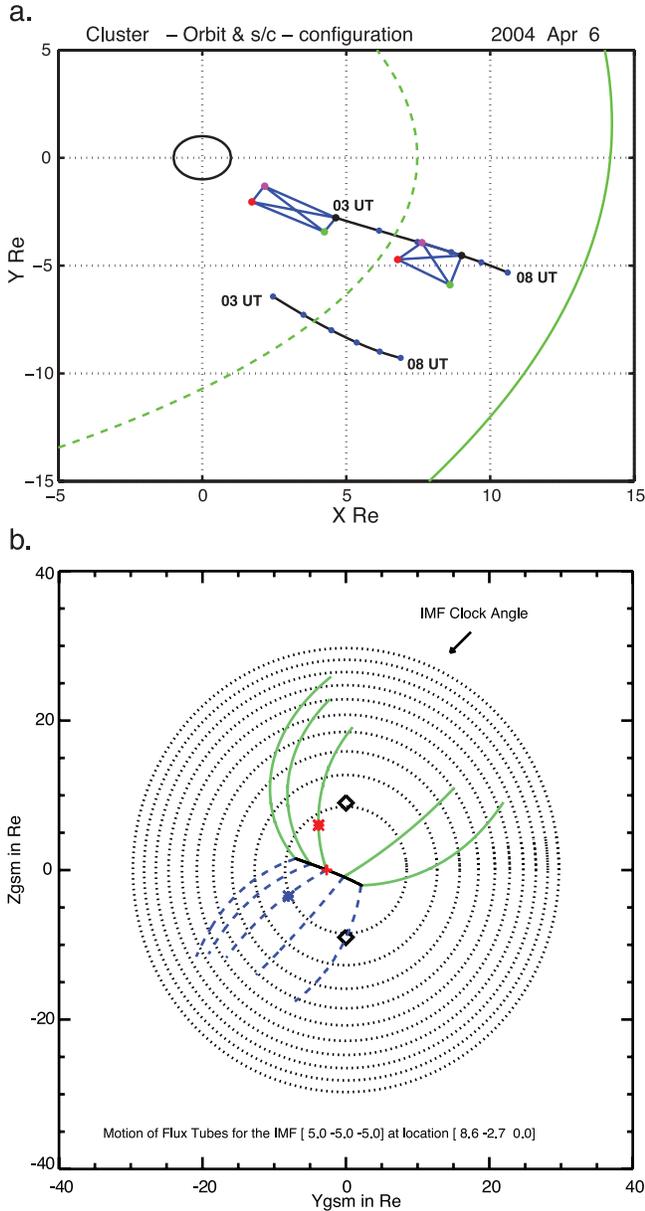
a.

b.

Figure 1. (a) Cluster s/c1 and Double Star TC-1 tracks in GSM coordinates for the interval 0300 to 0800 UT on 6 April 2004. The Cluster orbit also shows two spacecraft configurations (scaled up by a factor X50). Each orbit has hour markers. Model field lines are shown for the projection into the X, Z plane and cuts through the bow shock and magnetopause are shown for the X, Y plane. (b) The result from the Cooling model is projected in the YZ plane, looking earthward from the Sun. Concentric dotted circles are magnetopause radii at 5 R_E intervals along the X direction, with the innermost representing X = 5 R_E. The diamonds represent the cusps for a MP standoff distance of 9 R_E. The triangle is the position of Double Star and the square, Cluster. Pairs of open reconnected flux tubes are initiated along the merging line (dot-dashed), with the motion of each calculated for 500 s. The IMF is indicated by the arrow in the upper right-hand corner but becomes more dawnward during the event.

motions by multispacecraft analysis [*Dunlop et al.*, 2005], since the profiles are similar and each identified FTE is sampled by all Cluster spacecraft. The motion of the flux tubes, although consistently northward at Cluster, appeared to be sensitive to prevailing conditions (the changing IMF clock angle) and precise spacecraft locations, as would be implied by the fan of tracks in Figure 1b. The flux tubes connected to the southern cusp have southwest motion which is confirmed by de-Hoffmann-Teller analysis on the FTEs at TC-1. Some FTEs seen simultaneously at each location represent coincidently generated flux tube pairs [*Dunlop et al.*, 2005], as is suggested by the tracks passing through TC-1 and Cluster in Figure 1b. Moreover, fewer and weaker FTEs are observed by TC-1 since it appears it lies on the edge of the implied set of flux tube tracks.

[12] All these FTE signatures were found to correspond closely to the Cooling model calculation: from the timing of FTE occurrence and the motions, the X line position was shown to be centrally located between the TC-1 and Cluster locations. The observations therefore confirm that quasi-steady or sporadic reconnection was ongoing during the event, where Cluster and TC-1 were nearly equidistant from the X line, suggesting that a single reconnection site occurs near the subsolar point.

[13] Figure 2 (fifth to seventh panels) shows the ion energy spectra for the TC-1 spacecraft and the Cluster 3 spacecraft, and the energy averaged pitch angle distribution for Cluster 3, as taken from the HIA-CIS detector. Cluster 3 is chosen since it shows the most typical plasma distributions and is representative of the other Cluster spacecraft. Exits into the magnetosheath are clear both in the plasma and magnetic field data, and indicate magnetopause crossings at 0415 UT for TC-1 and 0433 UT for Cluster. Because of its southerly and duskward location, there is a much lower local magnetic shear across the magnetopause at TC-1. The ion data from TC-1 shows a number of partial crossings of the boundary layer before final entry into the magnetosheath and closer analysis (not shown here) reveals that there is a well developed boundary layer at the TC-1 magnetopause traversal around 0415 UT. The spectra shown do show a smooth transition between magnetosheath and magnetospheric plasma around this time. For Cluster, the boundary layer appears to be less developed so that the magnetopause crossings show more distinct magnetospheric and magnetosheath populations in both the spectra and the pitch angles. We investigate the boundary layer properties further below. The FTEs are also apparent in the ion data shown in Figure 2, superimposed on the main transition into the magnetosheath as transient, mixed plasma signatures. There is also some evidence of field aligned populations on opened flux near the magnetopause crossings (bursts of near zero pitch angle flux after 0415 UT in Figure 2 (fifth to seventh panels)). The low magnetic shear across the magnetopause at TC-1 further confirms that the FTEs are not expected to be locally generated at TC-1, whereas, despite the high local magnetic shear at Cluster, the confirmed FTE motions were previously shown to originate at the low latitude merging site. This limit on the local extent of the boundary layer, measured at about 5 R_E from the low-latitude X line, either north or south, is also demonstrated from the bulk hot ion parameters, calculated from the HIA data and shown in Figure 3. The Cluster velocities, in
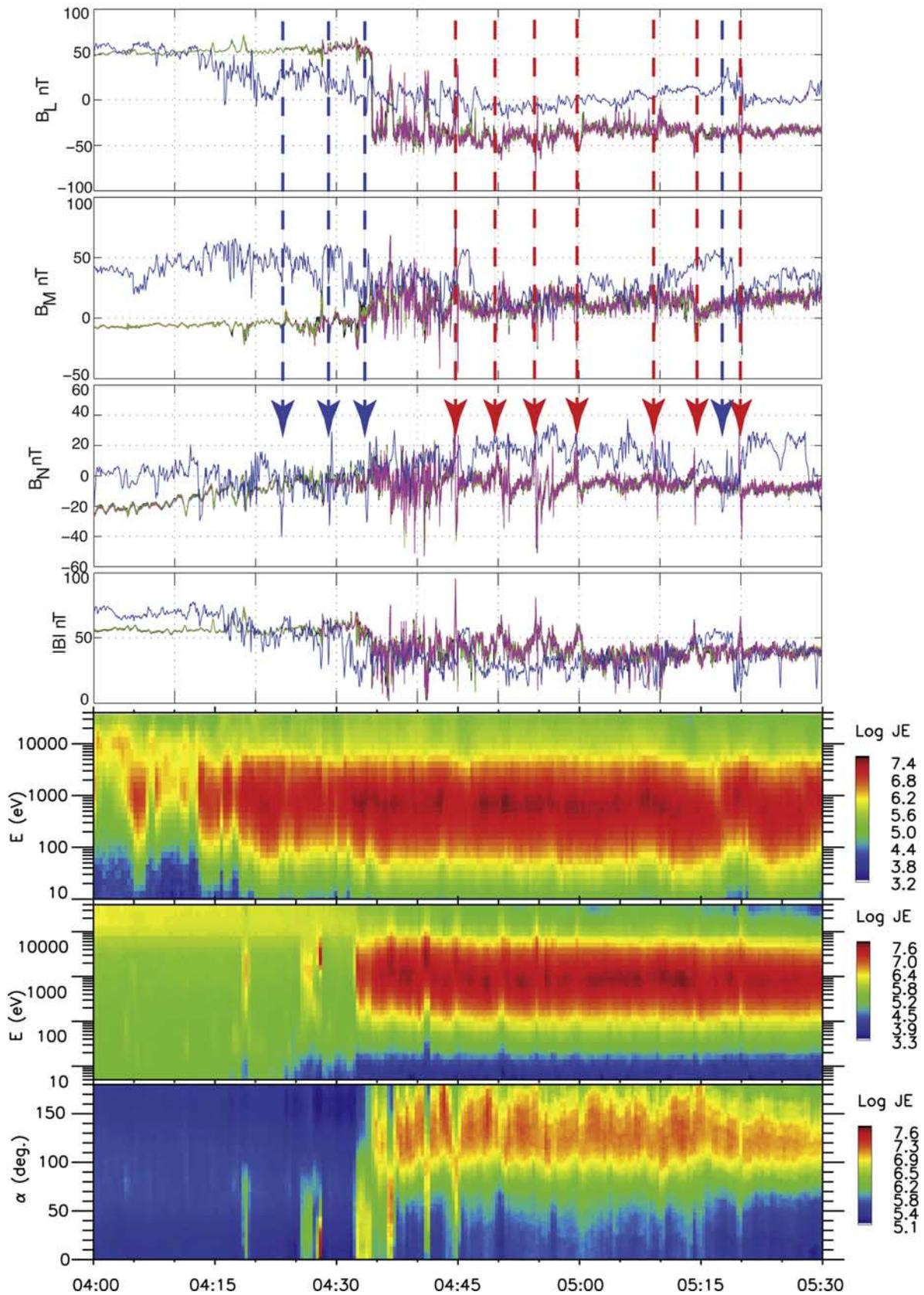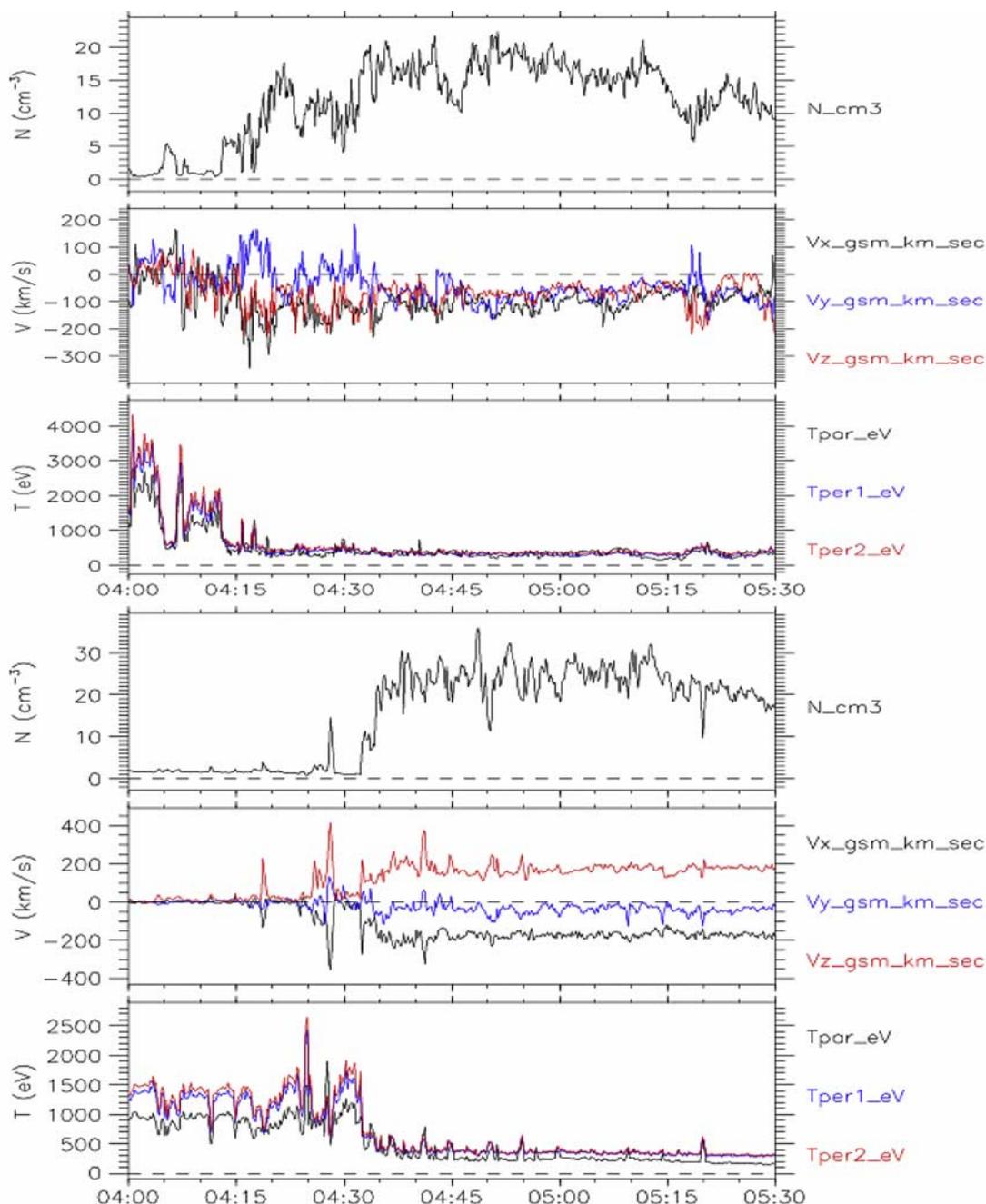
Figure 2

Figure 3. The ion bulk parameters (density, n, velocity, V, and temperature, T) are presented for TC-1 (first to third panels) and Cluster 3 (fourth to sixth panels). The Walen relation is not closely satisfied for the ion flows seen in the TC-1 data in the boundary layer between 0415 and 0430 UT.

particular, show well separated magnetosheath and magnetospheric regimes, whereas the TC-1 velocities are rather turbulent and show some evidence of local ion jets, distinct from the magnetosheath flow.

[14] Figure 4 shows the electron distributions for the same interval as Figure 2, also for TC-1 and Cluster 3, which broadly confirm the results taken from the ions. Figure 4a (first and fourth panels) present spectrograms of spin-

Figure 2. (first to fourth panels) A multispacecraft plot of the magnetic field in LMN (MVA) coordinates, taken from TC-1 (blue), and the four Cluster spacecraft (black, red, green, magneta). The analysis of Cluster gives [n = 0.72 0.16 0.68, m = −0.38 −0.72 0.58, l = −0.58 0.67 0.46] and TC-1 gives [n = 0.23 −0.68 −0.69, m = −0.68 −0.63 0.39, l = 0.70 −0.38 0.61] (components in GSM). Clear FTEs are observed at Cluster (all spacecraft) with +/− polarity. The FTEs at TC-1 are less clear, but most have −/+ (reverse) polarity. (fifth to seventh panels) Spin-integrated differential ion energy flux for TC-1 and Cluster 3, respectively, and the ion pitch angle distribution for Cluster 3 from the HIA sensor.
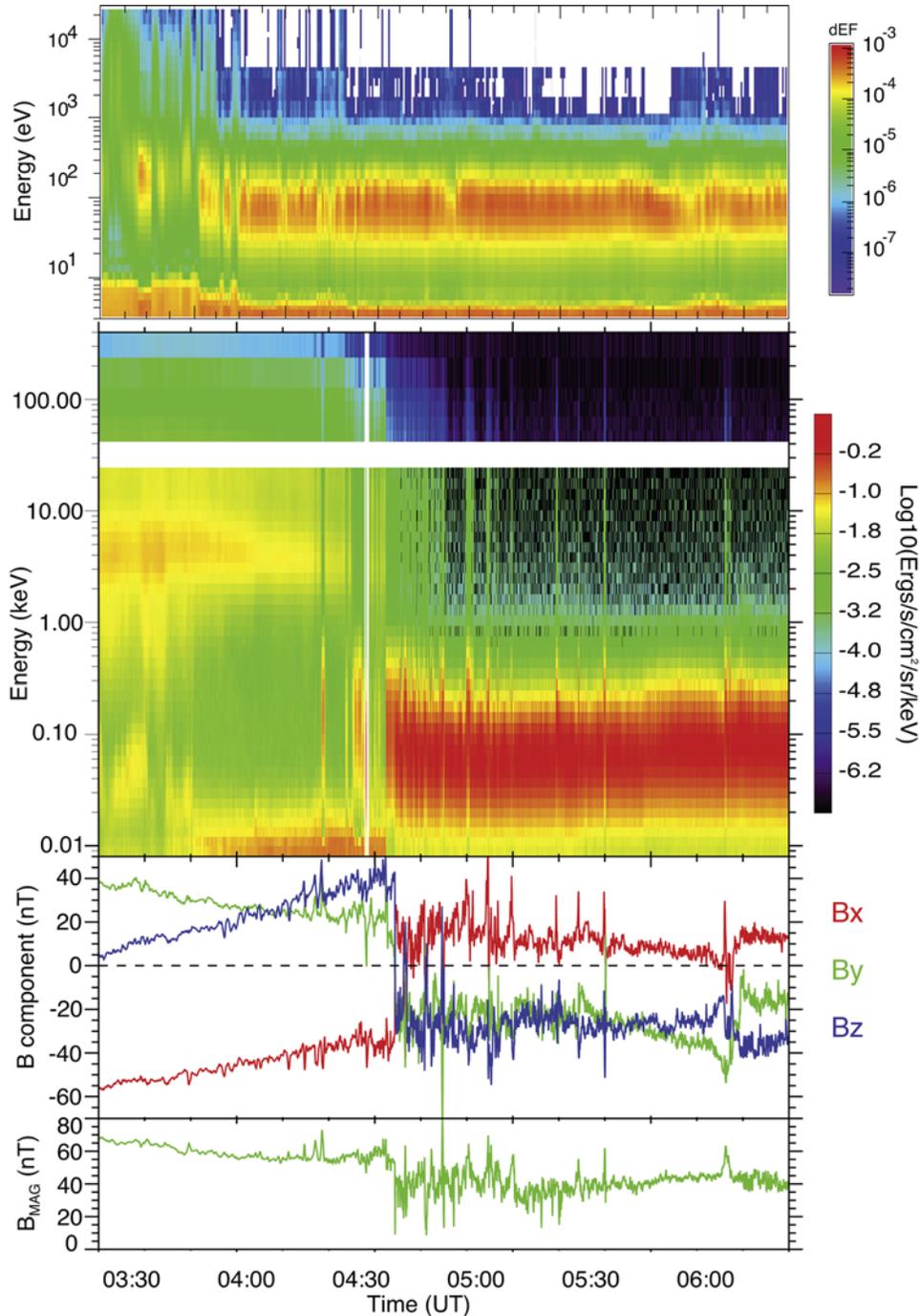
Figure 4a. Summary of the extended electron distribution from the PEACE/Rapid measurements of spin-integrated, differential energy flux for the interval shown for Cluster 3 and TC-1, respectively. The magnetic field from Cluster 3 is also shown.

averaged, differential electron energy flux from the PEACE instrument on TC-1 (Figure 4, first panel) and the combined data from the PEACE instrument and the RAPID-IES sensor from Cluster 3 (Figure 4, fourth panel). Together, these measure an energy range extending to 400 keV. The magnetic field data from the FGM instrument on TC-1 (Figure 4a, second and third panels) and Cluster 3 (Figure 4a, fifth and sixth panels), respectively, are shown again for guidance. The FTE signatures are

clearly seen, particularly for Cluster, and show a mixed distribution of heated magnetosheath and magnetospheric plasmas, extending to the energetic electron energies. Similarly to the ions, the magnetopause crossings at Cluster show sharp boundaries with well separated magnetosheath and magnetospheric distributions, even during the partial exits before 0435 UT, suggesting a narrow boundary layer. The magnetopause current at Cluster, corresponding here to the B_Z reversal, is only encountered at the final exit into the
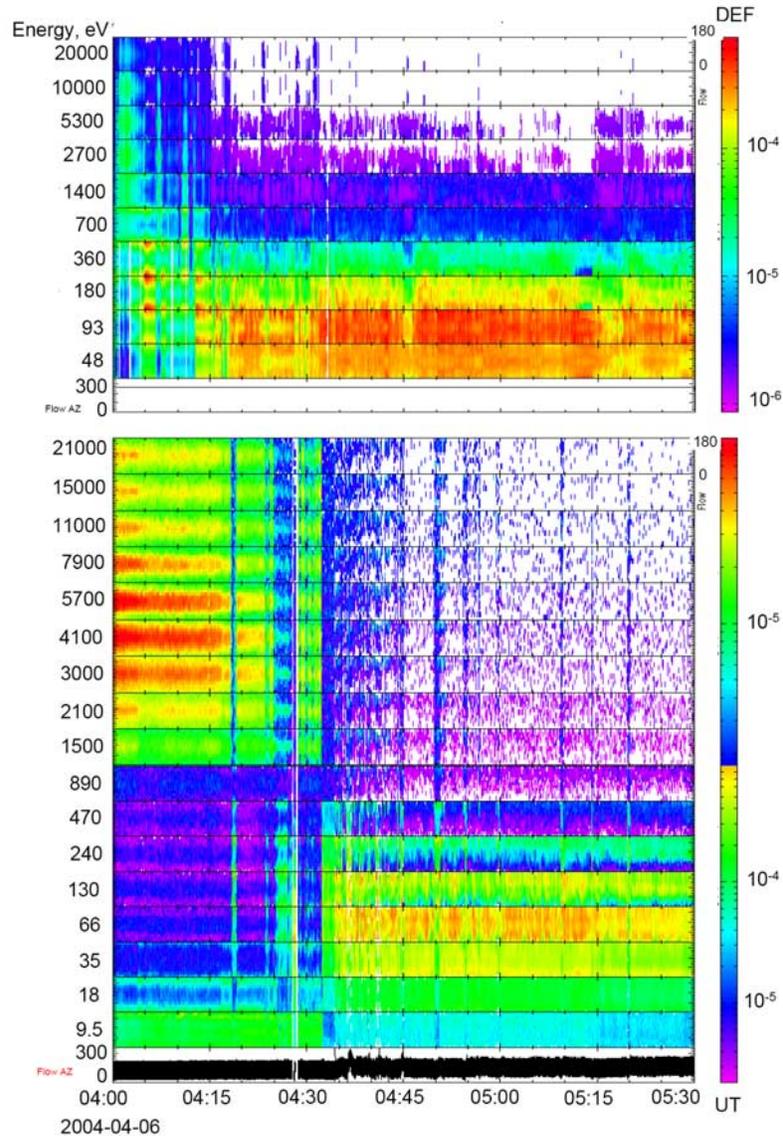
Figure 4b. The thermal electron pitch angle distributions from the PEACE instrument. Stacked energy plots (top) for TC-1 and (bottom) for Cluster3. The Cluster data are binned at a higher resolution in energy. The pitch angles run from 0 to 180°, from the bottom to top of each panel.

magnetosheath. At TC-1 the boundary layer appears to be thicker, and, as for the ion distribution, shows a more gradual change from magnetospheric to a magnetosheath-like distribution.

[15] These facts have significance for the relative space-craft positions on the magnetopause, as shown in Figure 1, and suggest a dawn-dusk asymmetry, perhaps linked to the local magnetic shear angle. This is lower at the TC-1 location as is clear from the change in field direction at the magnetopause crossings around 0430 UT in Figure 2 (the inferred value of the angle between the magnetosheath and magnetospheric fields, lies close to that inferred from the model field and a mean IMF direction for both the TC-1 and Cluster locations). As discussed earlier and as analyzed in *Dunlop et al.* [2005], these particular spacecraft locations allowed both the north and south reconnection region to be quantitatively mapped simultaneously, thus fixing the location of the reconnection line as nearly equidistant from each

spacecraft location. The limited boundary layer at Cluster, lying more then 5 R_E north of the X line, is perhaps understandable, therefore, in terms of a limited, latitudinal extent of the LLBL. The TC-1 result, that a more extensive boundary layer occurs south of the reconnection line, is less clear, however, and appears to be related only to the lower shear angle and more dawnward location. Below we investigate the details of the electron properties to show these differences further.

[16] Figure 4b shows the details of the electron pitch angle distributions, and its dependence on energy, from the PEACE instrument on both TC-1 (Figure 4b, top) and Cluster 3 (Figure 4b, bottom), starting at 48 eV and 9.5 eV, respectively. These plots each show a stacked set of differential energy flux as a function of pitch angle (vertical direction), for the energy bins indicated by the center values. The pitch angle runs from 0 to 180° from bottom to top in each panel. The dominant flux is a locally
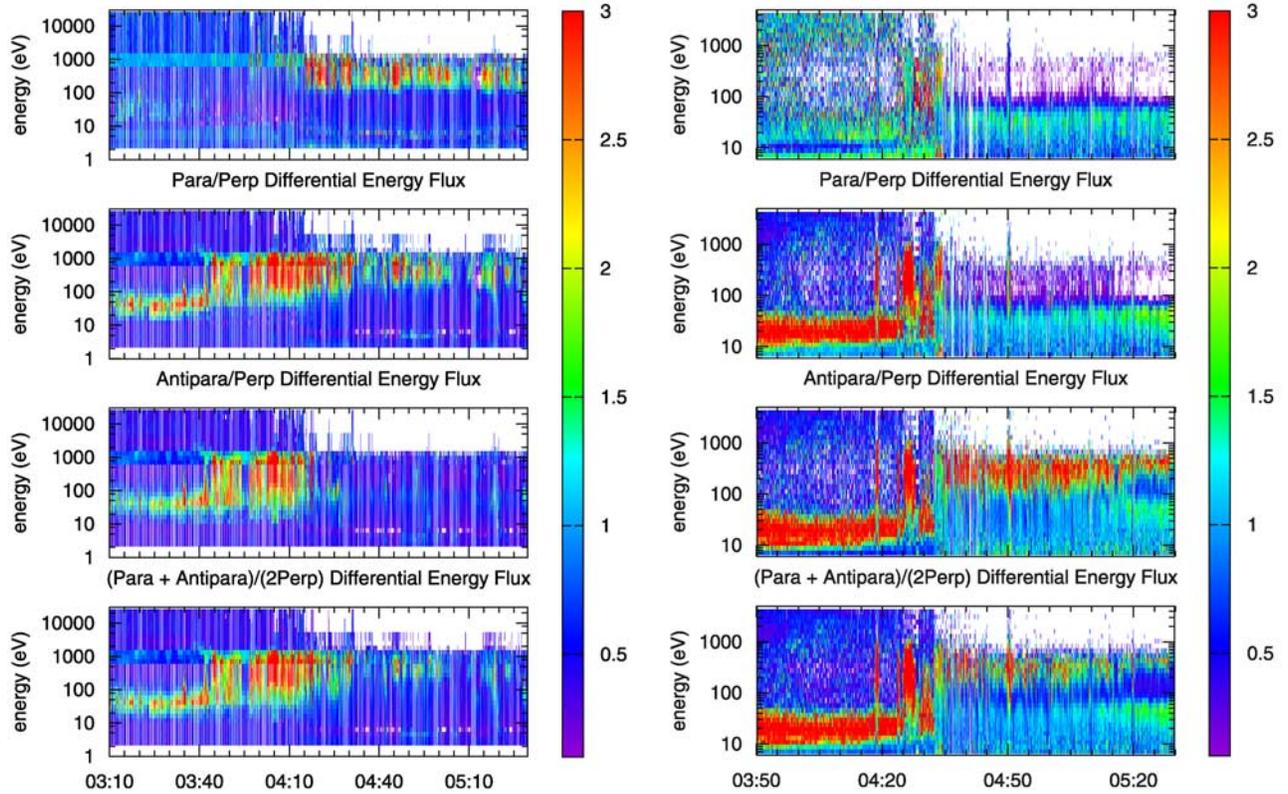
Figure 5a. Electron anisotropies from the PEACE-HEEA sensor on both (left) TC-1 and (right) Cluster 3 and for the interval indicated.

trapped distribution at 90° pitch angle at both locations and in addition shows a field-aligned population at low energies, throughout most of this interval. For Cluster, the trapped distribution lies at energised magnetosheath energies (ranging from 66 eV to 21 keV during the interval 0400–0435 UT). For TC-1 the trapped distribution is during the period 0400–0415 UT at energies ~3–20 keV. Antiparallel flux (outflowing electrons) is observed at each FTE, but also outside the FTEs, in the energy range 130–470 eV for Cluster. For TC-1, the distribution shows both a field-aligned population below about 1 keV and a locally trapped population above 1 keV, which disappear as the boundary layer is traversed. At energies above 1 keV, the 90° pitch angle distribution is dominant. A bistreaming population at (heated) magnetosheath energies is consistent with recently closed field lines [*Onsager et al.*, 2001; *Lavraud et al.*, 2006] (previously opened flux), whereas the trapped population at high energies is consistent with a magnetospheric plasma distribution in the dayside plasma sheet. TC-1 sees the bidirectional population before 0430 UT and just after the magnetopause crossing at 0415 UT. After 0430 UT, the TC-1 distribution evolves into an isotropic, convecting, magnetosheath distribution at the lower energies, whereas Cluster detects an outflowing population at energies 130–470 eV in the magnetosheath. The TC-1 distribution is appears to be more field aligned at the higher (magnetospheric) energies.

[17] These electron distributions may be investigated further in terms of the electron anisotropy (ratios of parallel to perpendicular and parallel to antiparallel differential energy fluxes) and these are shown in Figure 5 (note that

the time intervals chosen, 0310–0530 UT for TC-1 and 0350–0530 UT for Cluster, are slightly different to the previous plots in order to position the magnetosphere/magnetosheath transition more centrally in each case). In Figure 5a, the anisotropy is calculated as a function of energy and time. The TC-1 anisotropy shows that the boundary layer population at magnetosheath energies is primarily bidirectional (the ratio, parallel/perpendicular ~1, while the ratio field aligned/perpendicular ~3) until the final magnetopause crossing at ~0415 UT. We should note that actually, the region either side of the boundary layer on TC-1 is now seen during the interval 0340–0410 UT. The magnetospheric side is missing on the previous plots, as they start from 0400 UT. Thus, the wider extent of the boundary layer in TC-1, is now confirmed by the anisotropy ratios in Figure 5a, which highlight the dominant, bistreaming population encountered between about 0340 and 0420 UT, for TC-1, whereas a (less dominant) bidirectional population is contained in the brief intervals near the magnetopause crossings (around 0418 and 0425 UT), for Cluster. The FTE signatures (identified in Figure 2) contain dominant field parallel populations, consistent with out-flowing electrons on south connected opened flux. The Cluster anisotropy also shows a more extensive field antiparallel population in the magnetosheath, again consistent with outflowing electrons on north connected opened flux. These anisotropies are therefore consistent with the scenario discussed above, which implied a local time dependence linked to the IMF orientation, since they broadly support the existence of an old (established)
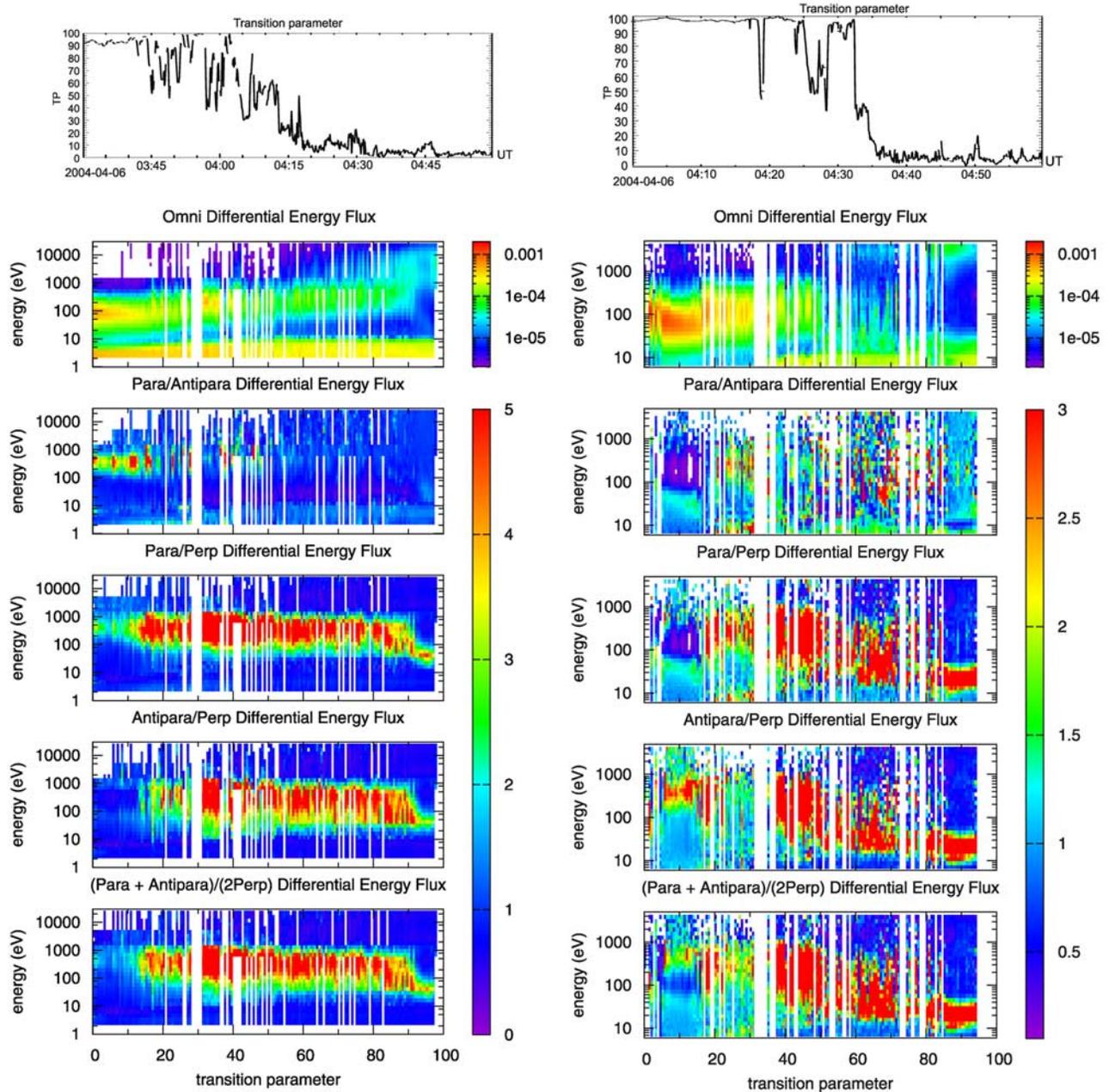
Figure 5b. (first panel) Transition parameter fits and (second to sixth panels) the sorted electron anisotropies as a function of the transition parameter for (left) TC-1 and (right) Cluster 3.

reconnection layer containing bidirectional flux and showing strong dawn-dusk asymmetry north and south of the X line.

[18] We can also investigate the electron anisotropy using the natural ordering of the electron distribution through the magnetosphere to magnetosheath transition. A method, designed to resort the data according to position in the boundary layer, was devised by *Hapgood and Bryant* [1992]. This uses a fit to the monotonic trend in the electron density and temperature in order to obtain a transition parameter (TP). This parameter is normalized to give zero for the low-temperature, high-density extreme of this fit (corresponding to magnetosheath populations) and 100 for the high-temperature, low-density extreme (corresponding

to magnetospheric populations). This ordering of the transition from the magnetosphere to the magnetosheath by the properties of the electron distribution was further interpreted by *Lockwood and Hapgood* [1997] as loosely representing the time elapsed since reconnection in an active boundary layer. It therefore can provide a technique for reordering the time series data according to positions through the boundary layer and takes out the effect of boundary motion relative to the spacecraft to a large degree. Figure 5b shows the transition parameter ordering for this event, for TC-1 (Figure 5b, left) and Cluster3 (Figure 5b, right) with the TP fits shown in Figure 5b (first panels). The TP analysis shows clearly how limited the boundary layer at Cluster is,

while the range of TP values at TC-1 shows a more extended coverage over all values. The resorted data shows the outflowing distributions in the magnetosheath range (TP = 0–15): a dominant parallel (antiparallel) population for TC-1 (Cluster). The bi-directional population in the boundary layers extends over TP = 15–80, for TC-1, whereas that for Cluster extends over TP = 30–50, and the field-aligned distribution is again shown to be less dominant. The FTE signatures overlap with the TP range over the boundary layer and therefore, although this is not inconsistent, they are rather hidden in this representation. In addition, the Cluster data is less well sorted than for TC-1.

3.2. Event of 4 January 2005

[19] The second Cluster and TC-1 conjunction occurred during the core interval 06 to 0800 UT, on the 4 January 2005 and has been briefly studied by *Wang et al.* [2007] in terms of a single, tailward moving flux tube, sampled simultaneously along its length by both Cluster and TC-1. Figure 6a shows the spacecraft configuration during the event in the same format as for Figure 1a. During the interval, the Cluster array moves about 2 R_E from high latitudes (initially at ~6 R_E north) and moves outbound, almost along the surface of the duskside magnetopause at about 1600 LT. At the same time TC-1 crosses the Cluster LT at midlatitudes, but still in the Northern Hemisphere, as indicated. The orbit segments are shown for the interval 0600–0900 UT and the Cluster configurations are scaled up by a factor of 5; the Cluster spacecraft separations being ~1100 km at this time. The TC-1 spacecraft is separated from Cluster by ~3 R_E in Z_{GSM}, but clearly lies close to the same radial position as Cluster. All five spacecraft are therefore expected to exit the duskside magnetosphere almost simultaneously, since all spacecraft lie at the same LT and at the same radial position, but with Cluster lying at higher latitudes. The main magnetopause exit actually occurred at ~0708 UT for all spacecraft (see later discussion of Figure 7). After this time, the solar wind conditions corresponded to a southward orientation of the IMF, but this followed a sudden turning from an initially northward orientation, just before 0700 UT [*Wang et al.* 2007]. This reversal of the IMF corresponded to the arrival of a Heliospheric Current Sheet (HCS) at the magnetopause and occurred just before the Cluster and TC-1 spacecraft moved from the magnetosphere into the magnetosheath. This event is of interest since it represents a close, five spacecraft sampling of the magnetopause boundary layer, which developed during the few minutes following a sudden switch on of dayside reconnection. It is also of interest since it corresponded to a period of turbulent and energetic solar wind and the plasma distributions were significantly energised into the high energy regime (>30 keV).

[20] Figure 6b shows the Cooling analysis employed by *Wang et al.* [2007], which interpreted the observed FTE motion in terms of a tilted, low-latitude X line generating an inclined flux tube moving duskward and tailward. The observed motion was consistent with the predicted tracks shown, which are similar at Cluster and TC-1, and the time delays between the Cluster and TC-1 FTE encounters suggested that the magnetosheath branch of the flux tube lay across the magnetopause in a northeasterly orientation. Figure 7 shows the multispacecraft magnetic field data

which contained these signatures, together with the hot ion measurements from the HIA instrument on TC-1 and Cluster 3 in the same format as for Figure 2. The magnetic field data are plotted in equivalent LMN coordinates using the MVA magnetopause normal, as for the previous event, at spin resolution to clarify the signatures, although the analysis has been carried out on recalibrated, high-resolution Custer data. The main magnetopause crossing at 0708 UT can be seen in the B_L component, although there is a partial exit into the magnetosheath at about 0705 UT, and timing analysis on this boundary suggests it represents a fast crossing at ~130 km/s. The magnetopause normal is consistent with this LT and latitude for Cluster. There are a number of other reentries into the boundary layer in the interval plotted, which imply that the spacecraft remain in the adjacent magnetosheath. It is remarkable that all five spacecraft traces are closely similar throughout the interval, which arises from the similar locations relative to the magnetopause surface. The individual crossings show similar timescales for all spacecraft which implies that the gross magnetopause structure is very similar at all locations especially before 0725 UT. Analysis of the TC-1 crossings confirms that the magnetopause motion is similar to that found for Cluster.

[21] For the reconnection signatures, the first red dashed line and solid blue line mark the FTE, seen first at Cluster then TC-1, studied by *Wang et al.* [2007], who employed a number of techniques to compute the motion and orientation of the implied flux tube, and to reconstruct its geometry. The orientation was consistent with a draped flux tube, connected to the northern cusp, which was dragged duskward to cross first Cluster and then TC-1 at a lower-latitude position (more earthward) along its length. There are a number of other paired FTE encounters in the interval, and we mark these on the magnetic field plot by dashed red lines. Each of these has been studied and all show individual motions and implied flux tube orientations which are broadly consistent with each of the time delays observed between the Cluster array and TC-1. The orientation of the flux tubes in Z,Y_{GSM} has a dominant Z component, whereas the velocity has a dominant Y component, so that the precise orientation and direction of motion will be critical to the resulting time delay between each location. These observations are the first time flux tubes have been sampled at multiscale positions: through their cross section and along their length.

[22] The ion distributions, in Figure 7 (fifth to seventh panels), show the boundary layer crossings are indeed similar between Cluster 3 and TC-1 (note that the dropout in the TC-1 spectrogram between 0725 and 0731 UT is a mode change on the HIA instrument and is not real). This short interval suggests that the boundary layer is narrow since the magnetosheath and magnetospheric populations are distinct. Cluster 3 lies a little further out with respect to the magnetopause, and this is apparent later in the interval, after 0730 UT, when TC-1 may enter the inner boundary layer region while Cluster 3 remains in the outer boundary. Nevertheless, the magnetosheath signatures are similar for each spacecraft and show the FTE signatures, superimposed on the main magnetosheath distribution, as for the previous event. The energy averaged pitch angle distribution for Cluster 3 (bottom) shows a high degree of structure,
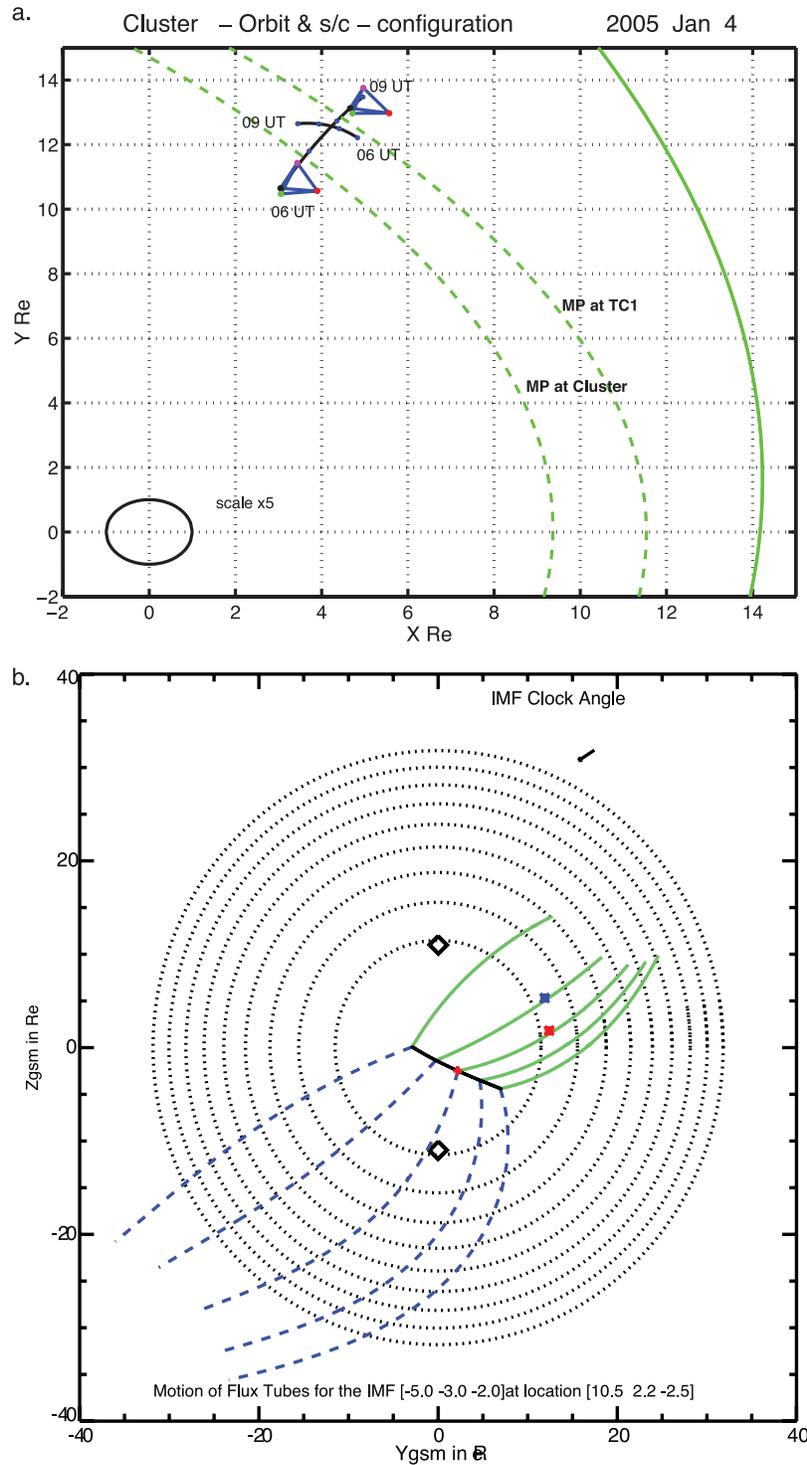
Figure 6. (a) As for Figure 1a in the X,Y plane, but for the event of the 4 January 2005. The orbital configuration is shown near the conjunction at 0700 UT, where Cluster lies about 4 R_E northward and TC-1 remains nearly equatorial. (b) The result from the Cooling model is shown in the same format as Figure 1b.

particularly in the later interval and partly relating to the turbulent nature of the magnetosheath following the HCS arrival, and this represents a rather unstable distribution which we discuss further below.

[23] We now turn again to the electron measurements. Figure 8a shows the electron distributions, with those from Cluster extended as before into the energetic energy range, for the overall interval, 0600–0800 UT. The magnetic field is also shown for the whole interval and now reveals that an
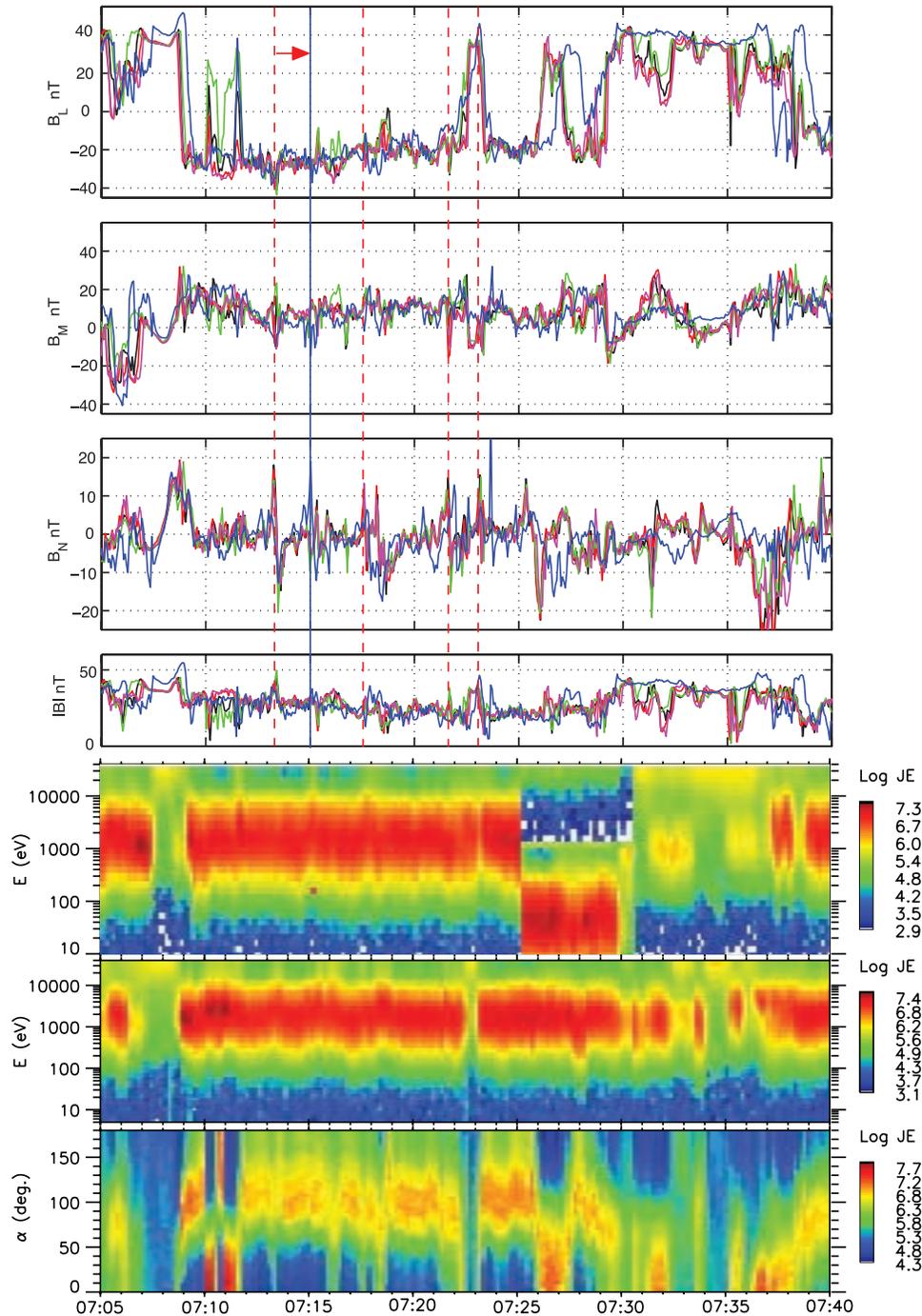
Figure 7. (first to fourth panels) A multispacecraft plot of the magnetic field in LMN (MVA) coordinates, in the same format as Figure 2. The analysis of Cluster gives [n = 0.65 0.71 0.26, m = −0.58 0.69 −0.43, l = −0.49 0.13 0.86], and the analysis of TC-1 gives [n = 0.72 −0.60 −0.36, m = 0.69 0.68 0.25, l = 0.09 −0.43 0.90] (components in GSE). The dashed lines refer to selected pairs of simultaneous FTEs at Cluster and TC-1. (fifth to seventh panels) Spin-integrated differential ion energy flux for TC-1 and Cluster 3, respectively, and the ion pitch angle distribution for Cluster 3 from the HIA sensor.

initial traversal into the magnetosheath occurs at around 0630 UT during northward IMF conditions on both the Cluster spacecraft and TC-1 (marked by the dashed red line). Following this low shear crossing, the spacecraft all remain in the adjacent magnetosheath in a strongly northward magnetosheath field, until the HCS arrives just before

0700 UT (timed by the convection time from ACE and marked by the dashed black line). The electron energy spectra show a number of partial traversals either side of the magnetopause throughout the interval 0600–0700 UT and no FTE signatures are observed. After this time there are two clear reentries into the magnetosphere, the last
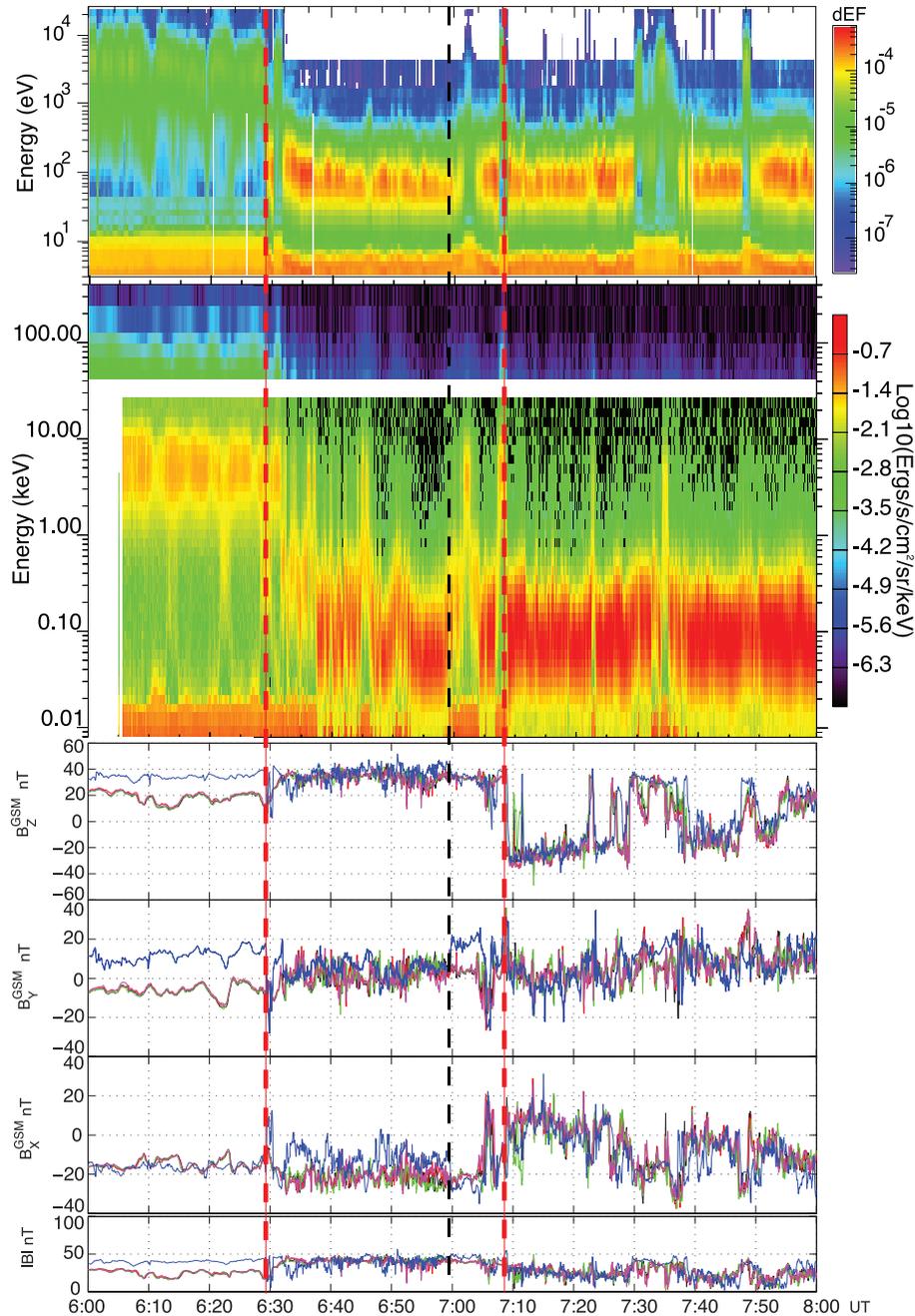
Figure 8a. Summary of the extended electron measurements of spin-integrated, differential energy flux from PEACE/Rapid, together with the magnet field in a similar format to Figure 3. The whole interval is shown to identify the development of the boundary layer and Cluster 1 is now used since this was the only Cluster spacecraft to take data over the whole interval.

marked by the high shear crossing discussed above. At each of these crossings the magnetopause exhibits properties of a rotational discontinuity and the Walen relation is well satisfied, suggesting the magnetopause becomes open at these times. The electron data also suggest that there is a limited or no boundary layer at TC-1 until the HCS reversal. Cluster, on the other hand, shows a well developed and complicated boundary layer, with significant mixing between the magnetosheath and magnetospheric plasma and significant fluxes at higher energies. Following 0700 UT it

appears that the boundary layer seen at the high Cluster latitudes becomes more limited in extent, after the onset of low latitude magnetic merging, and in contrast the boundary at TC-1 develops. This again suggests there is a rapid response of the global boundary layer structure to changes in the IMF orientation (transmitted to the magnetosheath). This event also shows a dependence on position on the magnetopause in a similar manner to the previous event, although here TC-1 and Cluster lie at similar locations, with Cluster at higher latitudes.
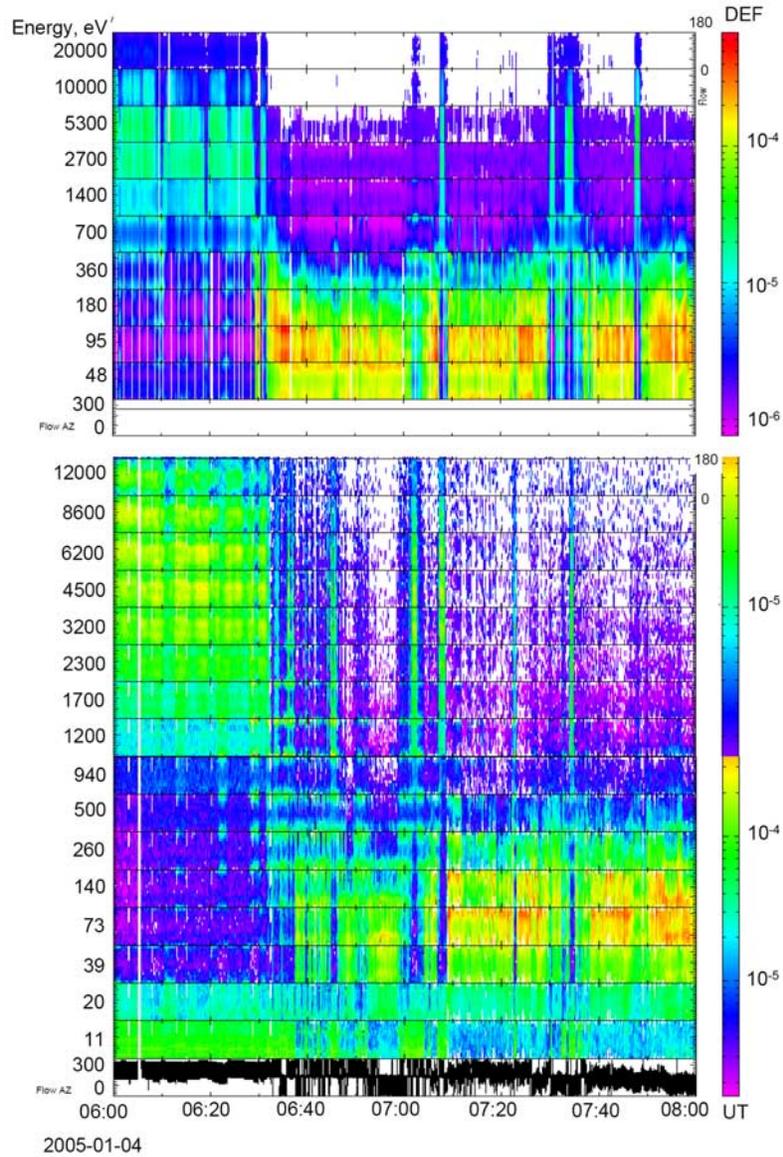
Figure 8b. The pitch angle distribution from TC-1 and Cluster 1, in the same format as for Figure 4b.

[24] The electron data confirms that all spacecraft remain very close to the magnetopause throughout the interval, resulting in many partial crossings and traversals through the boundary layer, and therefore they closely sample the magnetopause during the sudden onset of dayside reconnection. The pitch angle distributions are shown in Figure 8b for both TC-1 (Figure 8b, top) and Cluster 1 (same format as Figure 4b). These plots show a number of features. First at magnetosheath energies, it is clear that the turbulent nature after 0700 UT, seen in the ion data, is reflected in the electrons. Second, the Cluster distributions show a more structured distribution than TC-1 in the period 0600–0700 UT: at magnetosheath energies TC-1 shows an almost isotropic distribution, whereas Cluster shows temporal changes between locally trapped and more complex behavior, which appears to be correlated with proximity to the magnetopause. This behavior, which is linked to the strong northward IMF direction at this time, may be related to the

higher-latitude location of Cluster. In the boundary layer traversals, after 0630 UT (but before 0700 UT), bistreaming populations appear, which are most clear at mid energies, and are consistent with recently closed field lines, perhaps arising from a period of lobe reconnection [Bogdanova et al., 2008]. After 0700 UT the distributions become very similar between TC-1 and Cluster, in line with the midlatitude locations and development of a low-latitude X line. The boundary layer is in fact very active, containing energized plasma, during the whole interval for this event and the electron behavior on both sides of the magnetopause can be seen in more detail from the high-energy pitch angles.

[25] Figure 9a (first to fifth panels) shows the energy bins above 1 keV, and below 400 keV, using combined RAPID-IES and PEACE Cluster data, with the IES pitch angles at the top. The pitch angle distribution in the magnetospheric boundary layer before 0700 UT undergoes rapid changes
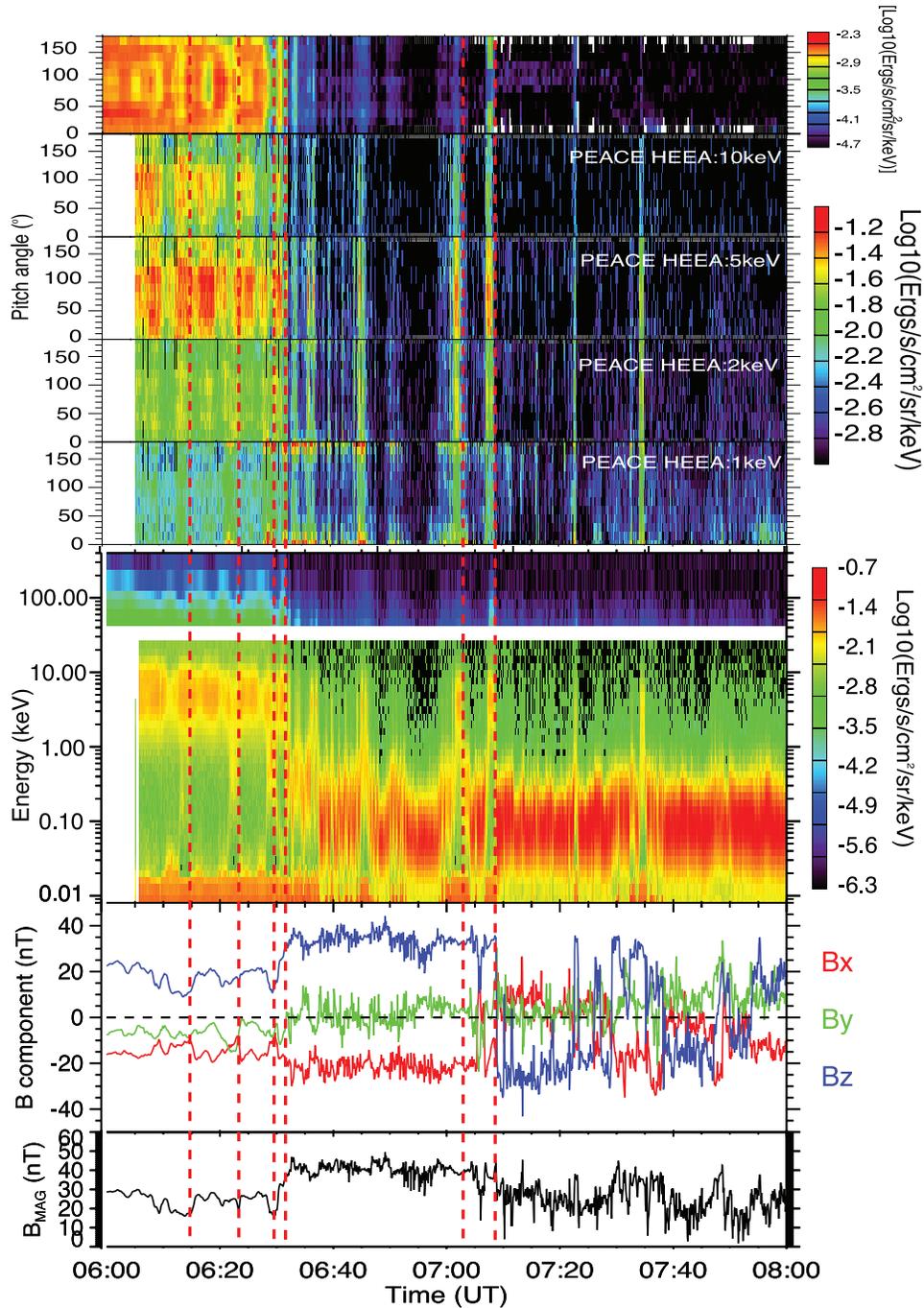
Figure 9a. (first to fifth panels) The Cluster energetic electron pitch angle distributions taken from the Rapid-IES instrument and the high-energy channels from the PEACE instrument, above 1 keV. (sixth to tenth panels) The differential flux and FGM data as in Figure 7a. Reentries to the magnetosphere are indicated by the dashed red lines.

from a nearly isotropic, to field-aligned, bistreaming distribution to a locally trapped distribution, in the energy range above 30 keV. By comparing these changes to the differential energy flux, it appears that the isotropic population is mostly associated with the region (dashed red lines) nearest to the magnetopause. In the magnetospheric boundary layer both bistreaming and 90° pitch angle distributions are seen. At lower energies the distributions are similar and these distributions correspond to the interval before the HCS

arrives, i.e., at low shear conditions (northward IMF) at the magnetopause. Figure 9a also shows that there are significant enhancements in the flux of energetic electrons observed at the later magnetopause crossings after 0700 UT (the time of the IMF reversal), where at the reentries into the magnetosphere the populations have developed into bidirectional pitch angle distributions in the magnetopause layer (marked by the dashed red lines). These later reentries into the magnetospheric boundary layer are therefore consistent
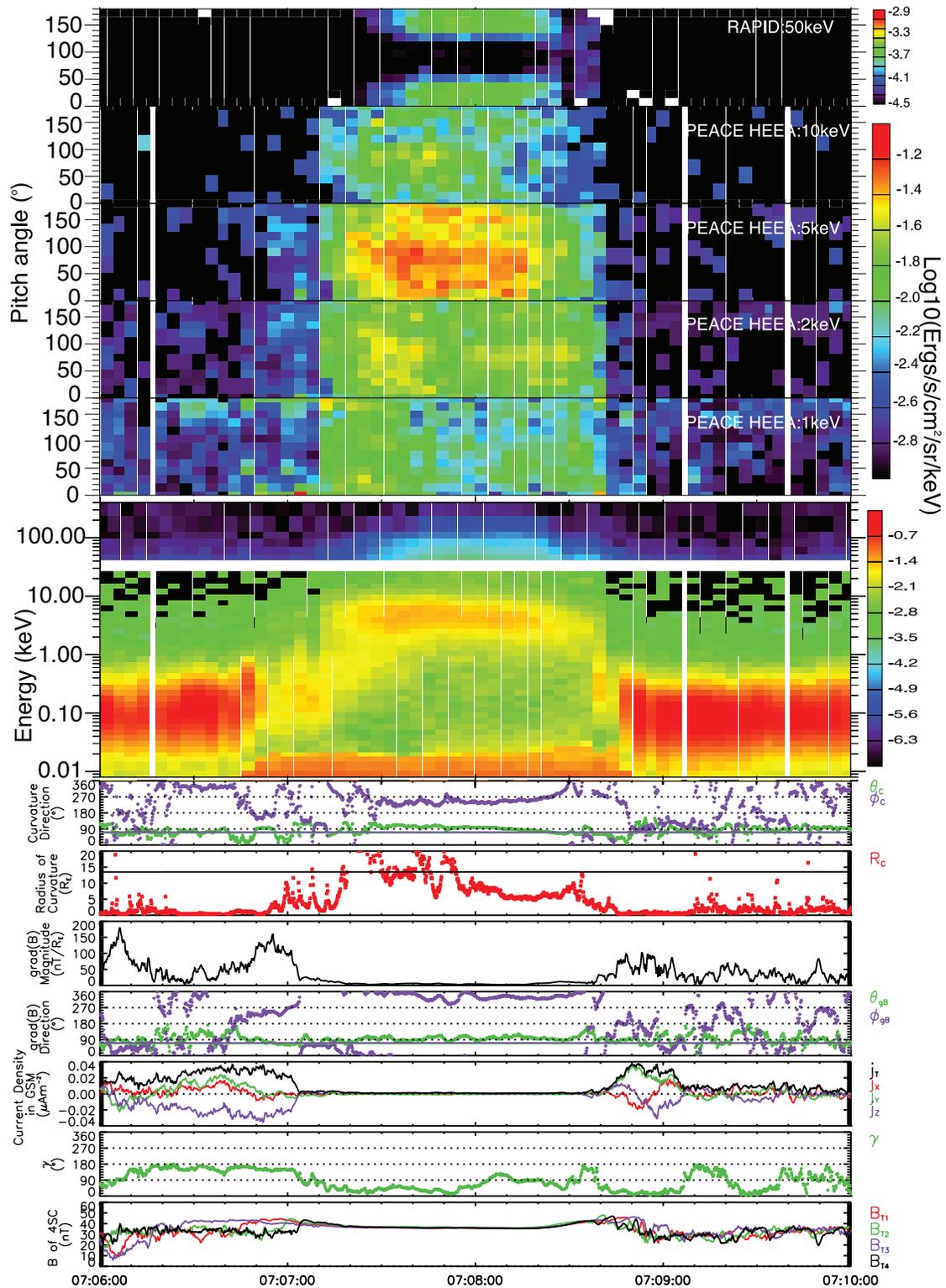
Figure 9b. Energetic electron, pitch angle distribution is shown in conjunction with the curvature analysis on the magnetic field for the short interval around the last magnetosphere reentry at 0708 UT.
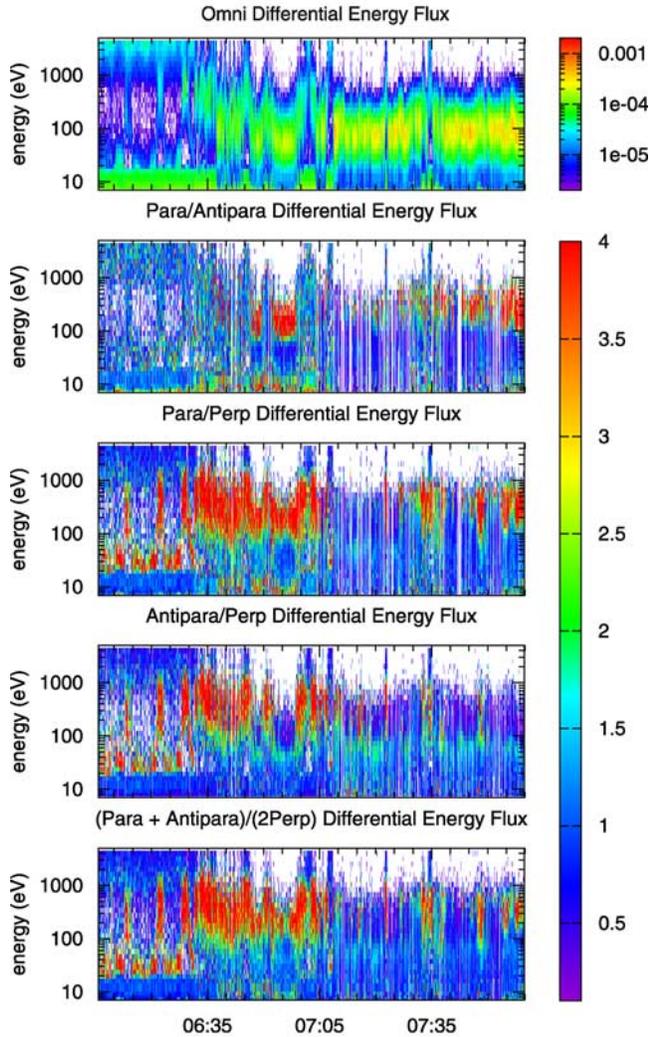
Figure 10a. The electron anisotropies for the PEACE-HEEA sensor on Cluster 1.

coincident with the current density. The value of gamma becomes close to 180° only outside the boundary layer (although the exit is a little confused). The plot shows that the field-aligned electrons are dominant in the energetic energy range and support a field-aligned current layer at the outer edge of the magnetopause.

[27] Figure 10 shows the electron anisotropies and transition parameter plots in a similar format as for Figure 5, for the thermal plasma, and for the interval 0600–0800 UT. These confirm that overall, the transition layer is much more limited for TC-1 (cf. the gaps in the TC-1 plot of anisotropy against transition parameter, in the range TP = 20–80). This result arises from two factors: first, the extensive sampling of the boundary layer comes from the early period between 0600 and 0700 UT, since there are only few reentries in the later period, and second, the electron distribution for TC-1 during this period (corresponding to northward IMF) has values of density and temperature which cluster into either the magnetospheric or magnetosheath range. We note here that the conditions appear very similar at all spacecraft locations, which all lie at closely similar positions relative to the magnetopause, as illustrated by the multispacecraft magnetic field plot in Figure 8a. All traces including TC-1 follow the in/out motions of the magnetopause after 0700 UT, so it is unlikely that the different transition ordering seen at TC-1 represents a more highly dynamic conditions there. Similar motions at TC-1 and Cluster were calculated at the magnetopause crossings by *Wang et al.* [2007].

[28] In contrast, therefore, the electron distribution for Cluster has a spread out range of density and temperature, which allows an even resorting of the energy anisotropy with respect to the TP. This is consistent with the distribution of differential energy flux over all energies during the boundary layer traversals, shown again in Figure 10a and as a function of TP in Figure 10b (first panels). Figure 10a showa that the dominant distribution in the boundary layer is a heated, bistreaming population, until entry into the magnetosheath. When resorted, we see that for Cluster the energetic boundary layer ranges across the full range of TP = 20–80 and shows an almost constant energization of the magnetosheath population to ~800 eV, mean energy. Such energies for the heated magnetosheath electrons are unusually high; the mean energy is usually ~500 eV maximum.

4. Discussion and Conclusions

[29] In this paper we have presented data during two magnetopause conjunctions between Cluster and the Double Star TC-1 spacecraft, which exhibit distinct properties in the dayside boundary layer during the operation of low latitude reconnection. We have used the combined, multiscale measurements of TC-1 and the four Cluster spacecraft to reveal these properties. During the first event, a series of oppositely directed flux transfer events (FTEs) are fed by a low-latitude reconnection line located midway between Cluster and TC-1. For the second event the spacecraft lie at the same duskward LT at northerly latitudes. The spacecraft repeatedly traverse the magnetopause, almost simultaneously, before and after a strong reversal in the IMF from northward to southward. The data suggest a sudden onset of reconnection for turbulent solar wind conditions. Following the IMF reversal correlated FTE signatures appear at all five

with the previous event for a low-latitude merging scenario, except that there is significant electron energization. The FTE signature which occurs at 0713:30 UT at Cluster and 0715 UT at TC-1 contains a field-aligned beam of energetic electrons (perhaps suggesting recently reconnected field lines on this flux tube). There is also a lower-energy (~5 keV) trapped population during the FTE encounter.

[26] Figure 9b shows the short interval surrounding the crossing at 0708 UT in conjunction with curvature and current analysis of the magnetic field [*Shen et al.*, 2007]. Figure 9b (first and second panels) shows the electron data and Figure 9b (third to ninth panels) shows the curvature, field gradient and current (inferred from curlB). The parameter gamma is the angle between the current and the magnetic field. The plot shows that at 0707 UT the current density becomes close to zero as the outer edge of the boundary is encountered. Inside this position the radius of curvature grows and becomes more stable as the spacecraft enters deeper into the magnetosphere. On exit back to the magnetosheath the same behavior is seen. The field gradient shows a strong pressure at the outside edge of the boundary,
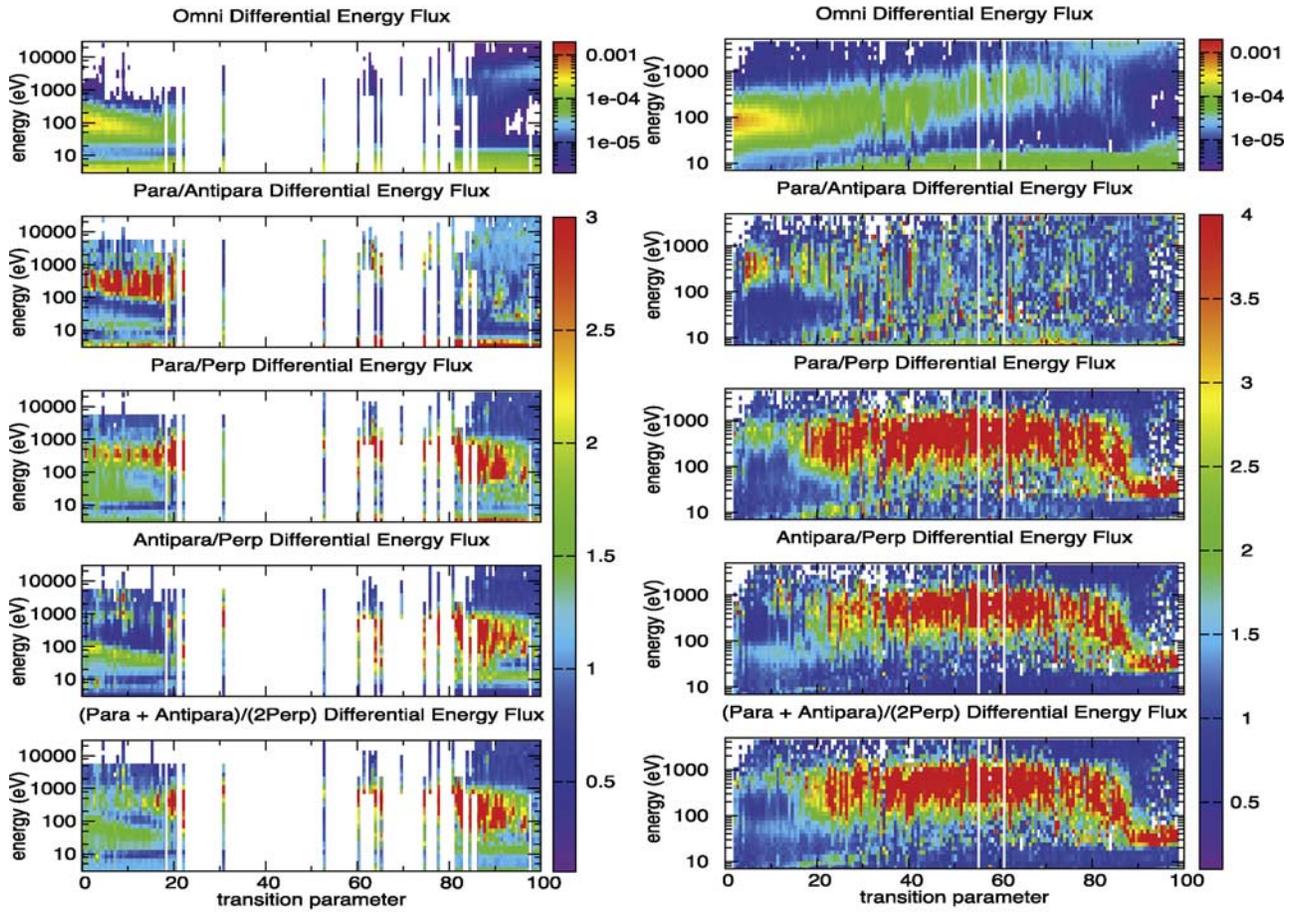
Figure 10b.   The sorted electron anisotropies with respect to the transition parameter for (left) TC-1 and (right) Cluster 1.

spacecraft, which are consistent with tilted, newly opened flux tubes moving duskward and tailward across the magnetopause and which are therefore shown to arise from the sudden formation of a near subsolar reconnection line within minutes of the IMF reversal.

[30]   In the first event, the spacecraft sample the magnetopause at similar positions north and south, almost equidistant from the subsolar X line at about 5 R_E. This results in the sampling of reconnected flux tubes at each location, which are remotely generated at the X line, together with crossings of the local magnetopause. The details of the plasma distributions show that outflowing electrons are consistently present on each flux tube and at the outermost edge of the magnetopause (most recently reconnected region at the magnetosheath boundary). An extensive boundary layer was maintained at TC-1, but not Cluster, however. Hence, for these duskward IMF conditions, we find a thicker boundary layer at the same distance south of the X line than north of it, although the structure is similar and consistent with the observed period of ongoing magnetic merging. For a dawnward location, south of the X line and for a duskward directed magnetosheath field, the local magnetic shear across the magnetopause is low as a result of the magnetospheric field orientation. The LLBL therefore appears to extend further south than its extent north of the X line, where the local magnetic shear is large and this

suggests the extent of the LLBL is asymmetric north and south. Although we have suggested here that local magnetic shear is associated with this asymmetric extent, we cannot rule out the possibility that a dipole tilt effect is changing the local magnetic boundary layer as a result of different magnetosheath flow properties (for example, affecting the pressure balance). It is true that the local magnetosheath signatures are more reminiscent of a plasma depletion layer at Cluster than at TC-1. This question requires further analysis of other events and will be pursued in a future paper.

[31]   In the second event, significant electron energization and the recent opening of the magnetopause layer at low latitudes, within minutes of reconnection onset, are clearly identified. All five spacecraft remain close to, or within, the magnetopause boundary layer for the 2 h period considered, which shows a complex and energized boundary layer at Cluster locations, which is largely absent at the lower latitudes of TC-1. Following the IMF reversal, this reconnection layer is seen to extend to TC-1 and becomes similar in character at both the Cluster and TC-1 sites. The spacecraft therefore monitor the development of a boundary layer structure following the IMF reversal and after the formation of a low-latitude X line dawnward of the spacecraft. In addition, the tilted flux tubes, which are sampled by all spacecraft at positions along their length, show a field-

aligned energetic electron population. Before the southward turning, locally trapped, isotropic and bistreaming populations of energetic electrons are seen at Cluster, extending up to 3–400 keV. There is a high degree of structure in the electron distributions, depending upon position within the layer: changing from isotropic near the magnetosheath boundary to bistreaming at deeper positions. During the same time (northward IMF), this layer appears to be more limited or absent at TC-1 at its lower-latitude location.

[32] Following the IMF reversal (a few minutes after reconnection onset), the electron population at Cluster develops as an energetic, field-aligned (bistreaming) distribution in the energetic energy range (above 30 keV) in the region adjacent to the magnetosheath boundary, whereas at low energies the population remains trapped. This probably indicates that these field lines are newly reconnected field lines. The behavior therefore becomes consistent with that expected, duskward of a low-latitude X line and the TC-1 distribution appears to be similar at this later time. The bistreaming energetic electron populations appear adjacent to the magnetopause current layer and the currents surrounding this distribution are field aligned. The local conditions for this second event are very similar at all spacecraft locations, as exhibited by the magnetic field profiles, which are similar for all five spacecraft. Thus, the changing structure observed is a result only of spacecraft locations and subsequently the sudden onset of dayside merging. Nevertheless, the precise relation of the energization to the boundary layer extent in this case is not clear and studies searching for other events are planned.

[33] The analysis of the boundary layer structure and its extent is assisted here by use of energy anisotropies derived from the electron distribution and by reordering the magnetopause transition to the TP. For Cluster, we have used the extended, measured energy range taken from the combined energetic and thermal electron instruments (ranging from a few to 400 keV). Multipoint measurements are needed to fully estimate the thickness of the boundary layer at different locations, as our observations show that the boundary layer is not uniform and the thickness depends on many factors. Thus, previous one-SC observations of the thickness of the boundary layer might be incorrect. A survey of other events which probe the extent and composition of the boundary layer under different conditions is underway.

References

Balogh, A., et al. (2001), The Cluster magnetic field investigation: Overview of in-flight performance and initial results, *Ann. Geophys.*, *19*, 1207–1217.

Berchem, J., and C. T. Russell (1984), Flux transfer events on the magnetopause: Spatial distribution and controlling factors, *J. Geophys. Res.*, *89*, 6689–6703, doi:10.1029/JA089iA08p06689.

Berchem, J., A. Marchaudon, M. Dunlop, C. P. Escoubet, J. M. Bosqued, H. Reme, A. Balogh, C. Carr, and Z. Pu (2008), Reconnection at the dayside magnetopause: Comparisons of global MHD simulation results

with Cluster and Double Star observations, *J. Geophys. Res.*, *113*, A07S12, doi:10.1029/2007JA012743.

Bogdanova, Y. V., A. Marchaudon, C. J. Owen, M. W. Dunlop, H. U. Frey, J. A. Wild, A. N. Fazakerley, B. Klecker, J. A. Davies, and S. E. Milan (2005), On the formation of the high-altitude stagnant cusp: Cluster observations, *Geophys. Res. Lett.*, *32*, L12101, doi:10.1029/2005GL022813.

Bogdanova, Y. V., et al. (2008), Formation of the low-latitude boundary layer and cusp under the northward IMF: Conjugated observations by Cluster and Double Star, *J. Geophys. Res.*, *113*, A07S07, doi:10.1029/2007JA012762.

Carr, C., et al. (2005), The Double Star Magnetic field investigation: Instrument design, performance and highlights of the first year's observations, *Ann. Geophys.*, *23*, 2713–2732, Ref-ID:1432-0576/ag/2005-23-2713.

Cooling, B. M. A., C. J. Owen, and S. J. Schwartz (2001), Role of magnetosheath flow in determining the motion of open flux tubes, *J. Geophys. Res.*, *106*, 18,763–18,775, doi:10.1029/2000JA000455.

Crooker, N. U. (1979), Dayside merging and cusp geometry, *J. Geophys. Res.*, *84*(A3), 951–959, doi:10.1029/JA084iA03p00951.

Dungey, J. W. (1961), Interplanetary magnetic field and the auroral zones, *Phys. Rev. Lett.*, *6*, 47–48, doi:10.1103/PhysRevLett.6.47.

Dunlop, M. W., A. Balogh, P. Cargill, R. C. Elphic, K.-H. Fornacon, E. Georgescu, F. Sedgemore-Schultess, and The FGM Team (2001), Cluster observes the Earth's magnetopause: Co-ordinated four-point magnetic field measurements, *Ann. Geophys.*, *19*, 1449–1462.

Dunlop, M. W., et al. (2005), Coordinated Cluster/Double Star observations of dayside reconnection signatures, *Ann. Geophys.*, *23*, 2867–2875.

Eastman, T. E., and E. W. Hones Jr. (1979), Characteristics of the magnetopsheric boundary layer and magnetopause layer as observed by IMP 6, *J. Geophys. Res.*, *84*(A5), 2019–2028, doi:10.1029/JA084iA05p02019.

Eastman, T. E., S. A. Fuselier, and J. T. Gosling (1996), Magnetopause crossings without a boundary layer, *J. Geophys. Res.*, *101*(A1), 49–58, doi:10.1029/95JA02757.

Escoubet, C. P., M. Fehringer, and M. Goldstein (2001), Introduction: The Cluster mission, *Ann. Geophys.*, *19*, 1197–1200.

Fazakerley, A. N., et al. (2005), The Double Star Plasma Electron and Current experiment, *Ann. Geophys.*, *23*, 2733–2756, Ref-ID:1432-0576/ag/2005-23-2733..

Fear, R. C., A. N. Fazakerley, C. J. Owen, A. D. Lahiff, E. A. Lucek, A. Balogh, L. M. Kistler, C. Mouikis, and H. Rème (2005), Cluster observations of boundary layer structure and a flux transfer event near the cusp, *Ann. Geophys.*, *23*(7), 2605–2620.

Fuselier, S. A., B. J. Anderson, and T. G. Onsager (1997), Electron and ion signatures of field line topology at the low-shear magnetopause, *J. Geophys. Res.*, *102*(A3), 4847–4863, doi:10.1029/96JA03635.

Gosling, J. T., M. F. Thomsen, S. J. Bame, R. C. Elphic, and C. T. Russell (1991), Observations of reconnection of interplanetary and lobe magnetic field lines at the high-latitude magnetopause, *J. Geophys. Res.*, *96*(A8), 14,097–14,106, doi:10.1029/91JA01139.

Hapgood, M., and D. Bryant (1992), Exploring the magnetospheric boundary layer, *Planet. Space Sci.*, *40*(10), 1431, doi:10.1016/0032-0633(92)90099-A.

Hasegawa, H., M. Fujimoto, T. D. Phan, H. Rème, A. Balogh, M. W. Dunlop, C. Hashimoto, and R. TanDokoro (2004a), Transport of solar wind into Earth's magnetosphere through rolled-up Kelvin-Helmholtz vortices, *Nature*, *430*, 755–758, doi:10.1038/nature02799.

Hasegawa, H., B. U. O. Sonnerup, M. W. Dunlop, A. Balogh, S. E. Haarland, B. Klecker, G. Paschmann, B. Lavraud, I. Dandouras, and H. Rème (2004b), Reconstruction of two-dimensional magnetopause structures from Cluster observations: Verification of method, *Ann. Geophys.*, *22*, 1251–1266.

Hu, Q., and B. U. O. Sonnerup (2003), Reconstruction of two-dimensional structures in the magnetopause: Method improvements, *J. Geophys. Res.*, *108*(A1), 1011, doi:10.1029/2002JA009323.

Johnstone, A. D., et al. (1997), PEACE: A plasma electron and current experiment, *Space Sci. Rev.*, *79*(1-2), 351–398, doi:10.1023/A:1004938001388.

Kessel, R. L., S.-H. Chen, J. L. Green, S. F. Fung, S. A. Boardsen, L. C. Tan, T. E. Eastman, J. D. Craven, and L. A. Frank (1996), Evidence of high-latitude reconnection during northward IMF: Hawkeye observations, *Geophys. Res. Lett.*, *23*(5), 583–586, doi:10.1029/95GL03083.

Lavraud, B., et al. (2002), Cluster observations of the exterior cusp and its surrounding boundaries under northward IMF, *Geophys. Res. Lett.*, *29*(20), 1995, doi:10.1029/2002GL015464.

Lavraud, B., M. F. Thomsen, M. G. G. T. Taylor, Y. L. Wang, T. D. Phan, S. J. Schwartz, R. C. Elphic, A. Fazakerley, H. Rème, and A. Balogh (2005a), Characteristics of the magnetosheath electron boundary layer under northward interplanetary magnetic field: Implications for high-

latitude reconnection, *J. Geophys. Res.*, *110*, A06209, doi:10.1029/2004JA010808.

Lavraud, B., A. Fedorov, E. Budnik, M. F. Thomsen, A. Grigoriev, P. J. Cargill, M. W. Dunlop, H. Rème, I. Dandouras, and A. Balogh (2005b), High-altitude cusp flow dependence on IMF orientation: A three-year Cluster statistical study, *J. Geophys. Res.*, *110*, A02209, doi:10.1029/2004JA010804.

Lavraud, B., M. F. Thomsen, B. Lefebvre, S. J. Schwartz, K. Seki, T. D. Phan, Y. L. Wang, A. Fazakerley, H. Rème, and A. Balogh (2006), Evidence for newly closed magnetosheath field lines at the dayside magnetopause under northward IMF, *J. Geophys. Res.*, *111*, A05211, doi:10.1029/2005JA011266.

Le, G., C. T. Russell, J. T. Gosling, and M. F. Thomsen (1996), ISEE observations of low-latitude boundary layer for northward interplanetary magnetic field: Implications for cusp reconnection, *J. Geophys. Res.*, *101*(A12), 27,239–27,249, doi:10.1029/96JA02528.

Liu, Z. X., C. P. Escoubet, Z. Pu, H. Laakso, J. K. Shi, C. Shen, and M. Hapgood (2005), The Double Star Mission, *Ann. Geophys.*, *23*, 2707–2712, SRef-ID:1432–0576/ag/2005–23–2707.

Lockwood, M., and M. A. Hapgood (1997), How the magnetopause transition parameter works, *Geophys. Res. Lett.*, *24*(4), 373–376, doi:10.1029/97GL00120.

Lockwood, M., et al. (2001), Co-ordinated Cluster and ground-based instrument observations of transient changes in the magnetopause boundary layer during an interval of predominantly northward IMF: Relation to reconnection pulses and FTE signatures, *Ann. Geophys.*, *19*, 1589–1612.

Marchaudon, A., C. J. Owen, J.-M. Bosqued, A. N. Fazakerley, M. W. Dunlop, A. D. Lahiff, C. Carr, A. Balogh, and H. Rème (2005), Simultaneous Double Star and Cluster FTEs observations on the dawnside flank of the magnetosphere, *Ann. Geophys.*, *23*, 2877–2887.

McComas, D. J., S. J. Bame, P. Barker, W. C. Feldman, J. L. Phillips, P. Riley, and J. W. Griffee (1998), Solar wind electron proton alpha monitor (SWEPAM) for the Advanced Composition Explorer, *Space Sci. Rev.*, *86*, 563–612, doi:10.1023/A:1005040232597.

Onsager, T. G., J. D. Scudder, M. Lockwood, and C. T. Russell (2001), Reconnection at the high-latitude magnetopause during northward interplanetary magnetic field conditions, *J. Geophys. Res.*, *106*(A11), 25,467–25,488, doi:10.1029/2000JA000444.

Paschmann, G. (1979), Plasma structure of the magnetopause and boundary layer, in *Magnetopsheric Boundary Layers*, edited by B. Battrick, *Eur. Space Agency Spec. Publ., ESA SP 148*, 25.

Phan, T.-D., M. Oieroset, and M. Fujimoto (2005), Reconnection at the dayside low-latitude magnetopause and its nonrole in low-latitude boundary layer formation during northward interplanetary magnetic field, *Geophys. Res. Lett.*, *32*, L17101, doi:10.1029/2005GL023355.

Pu, Z. Y., et al. (2005), Double Star TC-1 observation of magnetic reconnection at the dayside magnetopause: A preliminary study, *Ann. Geophys.*, *23*, 2889–2895.

Pu, Z. Y., et al. (2007), Global view of dayside magnetic reconnection with the dawn-dusk IMF orientation: A statistic study for TC-1 and Cluster data, *Geophys. Res. Lett.*, *34*, L20101, doi:10.1029/2007GL030336.

Rème, H., et al. (2001), First multispacecraft ion measurements in and near the Earth's magnetosphere with the identical Cluster ion spectrometry (CIS) experiment, *Ann. Geophys.*, *19*, 1303–1354.

Rème, H., et al. (2005), The HIA instrument onboard the Tan Ce 1 Double Star near-equatorial spacecraft and its first results, *Ann. Geophys.*, *23*, 2757–2774, SRef-ID:1432-0576/ag/2005-23-2757..

Rijnbeek, R. P., S. W. H. Cowley, D. J. Southwood, and C. T. Russell (1982), Observations of reverse polarity flux transfer events at the Earth's dayside magnetopause, *Nature*, *300*, 23–26, doi:10.1038/300023a0.

Rijnbeek, R. P., S. W. H. Cowley, D. J. Southwood, and C. T. Russell (1984), A survey of dayside flux transfer events observed by ISEE 1 and 2 magnetometers, *J. Geophys. Res.*, *89*(A2), 786–800, doi:10.1029/JA089iA02p00786.

Russell, C. T., and R. C. Elphic (1978), Initial ISEE magnetometer results: Magnetopause observations, *Space Sci. Rev.*, *22*, 681–715, doi:10.1007/BF00212619.

Russell, C. T., and R. C. Elphic (1979), ISEE observations of flux transfer events at the dayside magnetopause, *Geophys. Res. Lett.*, *6*(1), 33–36, doi:10.1029/GL006i001p00033.

Shen, C., X. Li, M. W. Dunlop, Q. Q. Shi, Z. X. Liu, E. A. Lucek, and Z. Q. Chen (2007), New approach for magnetic field rotation analysis and the application, *J. Geophys. Res.*, *112*, A06211, doi:10.1029/2005JA011584.

Sibeck, D. G., et al. (1989), The magnetospheric response to 8-minute period strong-amplitude upstream pressure variations, *J. Geophys. Res.*, *94*(A3), 2505–2519, doi:10.1029/JA094iA03p02505.

Smith, C. W., J. L'Heureux, N. F. Ness, M. H. Acuña, L. F. Burlaga, and J. Scheifele (1998), The ACE Magnetic Fields experiment, *Space Sci. Rev.*, *86*, 613–632, doi:10.1023/A:1005092216668.

Smith, M. F., and M. Lockwood (1996), Earth's magnetospheric cusps, *Rev. Geophys.*, *34*(2), 233–260, doi:10.1029/96RG00893.

Song, P., C. T. Russell, R. J. Fitzenreiter, J. T. Gosling, M. F. Thomsen, D. G. Mitchell, S. A. Fuselier, G. K. Parks, R. R. Anderson, and D. Hubert (1993), Structure and properties of the subsolar magnetopause for northward interplanetary magnetic field: Multiple-instrument particle observations, *J. Geophys. Res.*, *98*(A7), 11,319–11,337, doi:10.1029/93JA00606.

Sonnerup, B. U. O., and L. J. Cahill (1967), Magnetopause structure and attitude from Explorer 12 observations, *J. Geophys. Res.*, *72*(1), 171–183, doi:10.1029/JZ072i001p00171.

Stone, E. C., A. M. Frandsen, R. A. Mewaldt, E. R. Christian, D. Margolies, J. F. Ormes, and F. Snow (1998), The Advanced Composition Explorer, *Space Sci. Rev.*, *86*(1–4), 1–22, doi:10.1023/A:1005082526237.

Twitty, C., T. D. Phan, G. Paschmann, B. Lavraud, H. Rème, and M. Dunlop (2004), Cluster survey of cusp reconnection and its IMF dependence, *Geophys. Res. Lett.*, *31*, L19808, doi:10.1029/2004GL020646.

Wang, J., et al. (2007), TC1 and Cluster observation of an FTE on 4 January 2005: A close conjunction, *Geophys. Res. Lett.*, *34*, L03106, doi:10.1029/2006GL028241.

Wang, Y. L., R. C. Elphic, B. Lavraud, M. G. G. T. Taylor, J. Birn, C. T. Russell, J. Raeder, H. Kawano, and X. X. Zhang (2006), The dependence of flux transfer events on solar wind conditions from three years of Cluster observations, *J. Geophys. Res.*, *111*, A04224, doi:10.1029/2005JA011342.

Wild, J. A., et al. (2005), Simultaneous in-situ observations of the signatures of dayside reconnection at the high- and low-latitude magnetopause, *Ann. Geophys.*, *23*, 445–460.

Wild, J. A., S. E. Milan, J. A. Davies, M. W. Dunlop, D. M. Wright, C. M. Carr, A. Balogh, H. Rème, A. N. Fazakerley, and A. Marchaudon (2007), On the location of dayside magnetic reconnection during an interval of duskward oriented IMF, *Ann. Geophys.*, *25*, 219–238.

Wilken, B., et al. (1997), RAPID: The Imaging Energetic Particle Spectrometer on Cluster, *Space Sci. Rev.*, *79*, 399–473, doi:10.1023/A:1004994202296.

————————

Y. V. Bogdanova, A. N. Fazakerley, A. Walsh, and J. Owen, Mullard Space Science Laboratory, University College London, Dorking RH5 6NT, UK.

C. M. Carr, Blackett Laboratory, Imperial College London, London SW7 2AZ, UK.

J. A. Davies and M. W. Dunlop, SSTD, Rutherford Appleton Laboratory, Chilton, Didcot OX11 0QX, UK. (m.w.dunlop@rl.ac.uk)

M. G. G. T. Taylor, C. P. Escoubet, and H. Laakso, ESA/ESTEC, Keplerlaan 1, NL-2200 AG Noordwijk, Netherlands.

Z.-X. Liu and C. Shen, Centre for Space Science and Applied Research, Chinese Academy of Sciences, Beijing 100080, China.

J. Wang and F. Pitout, Max-Planck Institut fur Extraterrestrische Physik, P. O. Box 1312, D-85741 Garching, Germany.

Z. Pu and Q.-G. Zong, School of Earth and Space Sciences, Peking University, Beijing 100871, China.

B. Lavraud and H. Rème, Centre d'Etude Spatiale des Rayonnements, 9 avenue du Colonel Roche, F-31028 Toulouse Cedex 4, France.

Q.-H. Zhang, UAPS, Polar Research Institute of China, 451 Jinqiao Road, Shanghai 200136, China.